

Performance of Repetitive Controller under Frequency Variation

A thesis

submitted in partial fulfilment

of the requirements for the degree

of

M.S.

in

Robotics and Intelligent Machine Engineering

at

School of Mechanical and Manufacturing Engineering

National University of Sciences and Technology

by

Usman Rashid

Supervisor

Dr. Mohsin Jamil



2015

Abstract

Repetitive controller is used in a wide range of application areas; grid connected inverters, multilink robotic manipulators, AC-DC power supplies of high precision equipment, etc. The focus of this thesis is the performance of repetitive controller under frequency variation. A brief introduction to repetitive controller is presented along with a review of major contributions by well known researchers working in this area. The performance of repetitive controller is analysed under frequency variation. Also, a number of solutions to improve its performance under frequency variation are explored. Finally, the findings of this thesis are validated by applying to a Two Level Grid Connected Converter.

Dedication

This thesis is dedicated to Dr. Mohsin Jamil and Dr. Robert W. Erickson.

Acknowledgements

This work is the result of support, guidance and nonstop push by Dr. Mohsin Jamil. I am forever grateful to him. I also owe thanks to Dr. Omer Gilan for his support and guidance.

I am greatly thankful to National University of Sciences and Technology (NUST) for giving me an Endowment Scholarship. Without the scholarship, this work would have been much harder to complete.

My special thanks to all the fellow research students of Advanced Control Systems Lab especially Rizwan Arshad and Shahab Shahid Khawaja. Their moral support has been a great help during times of frustration.

I also owe a huge debt of gratitude to my family for their continuous support.

Declaration

1. I understand what plagiarism is and am aware of the University's policy in this regard.
2. I declare that this thesis is my own original work. Where other peoples work has been used (either from a printed source, Internet or any other source), this has been properly acknowledged and referenced in accordance with departmental requirements.
3. I have not used work previously produced by another student or any other person to hand in as my own.
4. I have not allowed, and will not allow, anyone to copy my work with the intention of passing it off as his or her own work.

SIGNATURE:.....

Contents

1	Motivation, Objectives and Contributions	15
1.1	Motivation	15
1.2	Aims and Objectives	17
1.3	Contributions of Thesis	17
1.4	Organisation of Thesis	18
2	Introduction to Repetitive Control	19
2.1	Synopsis	19
2.2	Performance of Close Loop System	19
2.2.1	Disturbance Rejection	20
2.2.2	Reference Tracking	20
2.3	Internal Model Principle	21
2.4	Proportional Resonant Controller	22
2.4.1	Limitations of Proportional Resonant Controller	22
2.5	Repetitive Controller	23
2.5.1	Periodic Signal Generator	23
2.5.2	Structure of Repetitive Controller	26
2.5.3	Stability Analysis of Repetitive Control System	31
2.5.4	Stabilising Compensator $G_x(z)$	33
2.5.5	Odd Harmonic Periodic Signal Generator	36
2.6	Repetitive Controller under Frequency Variation	38
3	Repetitive Controller Robust to Frequency Variation	41
3.1	Introduction	41

3.2	Frequency Adaptive Repetitive Controller	41
3.2.1	Difficulties in Implementing Adaptive Repetitive Controller	43
3.3	Higher Order Repetitive Controller	44
3.3.1	Higher Order Periodic Signal Generator	44
3.3.2	Structure of HORC	48
3.3.3	Stability Conditions for HORC	49
3.3.4	Phase Lead Compensation for HORC	50
3.3.5	Higher Order Odd Harmonic Repetitive Controller	51
4	Robust High Order Repetitive Control of Two Level Grid Connected Converter	53
4.1	Introduction	53
4.2	Evaluation Criteria	56
4.3	Two Level Converter	58
4.3.1	Conventional PID Controller	60
4.3.2	Testing the PID Controller	60
4.4	Conventional Repetitive Controller	62
4.4.1	Analysis of Designed Controller	66
4.4.2	Testing the Conventional Repetitive Controller	67
4.4.3	Performance under Frequency Variation	68
4.5	2 nd Order Odd Harmonic Repetitive Controller	69
4.5.1	Modified Compensator	73
4.6	Testing the Performance	73
4.7	Comparison of Results	75
5	Conclusion and Future Work	76
5.1	Conclusion	76
5.2	Future Work	77
A	Derivation of Formulae	78
A.1	Close Loop System's Error	78
A.2	Discrete Periodic Signal Generator	79

A.3	Fourier Series Formulation	80
A.4	Sensitivity Function of Repetitive Control System	81
A.5	Stability Conditions for Phase Lead Compensator	83
A.6	Weights of Higher Order Generator	85
A.7	Stability of Higher Order Repetitive Controller	87
A.8	Phase Lead Compensator for HORC	89
B	Elucidation of Concepts	93
B.1	Input Output Stability	93
B.1.1	H_∞ Stability	93
B.1.2	Small Gain Theorem	94

List of Figures

1.1	Frequency response of the discrete periodic signal generator tuned at 50 Hz. . .	16
1.2	Magnitude frequency response of periodic signal generator in the neighbourhood of tuned frequency (50 Hz).	16
2.1	Block diagram of generic close loop control system.	20
2.2	Frequency response of proportional resonant controller. This controller is tuned at 50 Hz and its both gains are unity.	23
2.3	Structure of periodic signal generator.	24
2.4	Signal generation by discrete periodic signal generator. The signal generated is of 50 Hz. The top plot is the input to periodic signal generator. The bottom plot is the output.	25
2.5	Magnitude of the Fourier coefficients, i.e A_o and A_n , of saw-tooth signal of 50 Hz.	26
2.6	Frequency response of the discrete periodic signal generator tuned at 50 Hz. . .	27
2.7	Block diagram of generic close loop control system along with the plug-in repetitive controller.	28
2.8	Internal structure of plug-in repetitive controller.	28
2.9	Frequency response of a test 3^{rd} order plant. The gain margin is 17.3 and phase margin is 75.7.	29
2.10	Frequency response of the test 3^{rd} order plant with periodic signal generator added. The gain margin is -0.276 and phase margin is -0.428.	30
2.11	Frequency response of periodic signal generator with lowpass filter added.	31
2.12	Frequency response of lowpass filter.	31
2.13	Frequency response of $G_x(z)$ for various values of m. Note that both axes have linear scales.	35

2.14	Structure of odd harmonic periodic signal generator.	37
2.15	Frequency response of odd harmonic periodic signal generator.	37
2.16	An odd harmonic signal having period 50 Hz.	38
2.17	Magnitude frequency response of periodic signal generator in the neighbourhood of tuned frequency (50 Hz).	39
2.18	Magnitude frequency response of periodic signal generator in the neighbourhood of tuned frequency.	39
3.1	Block diagram of generic close-loop control system along with the frequency adaptive plug-in repetitive controller.	42
3.2	Frequency response of adaptive repetitive controller tuned at 50 Hz. As the frequency of reference/disturbance changes, its tuned frequency is shifted by changing its sampling frequency.	43
3.3	Magnitude frequency response of periodic signal generator in the neighbourhood of tuned frequency.	44
3.4	Structure of 3 rd order periodic signal generator.	45
3.5	Frequency response of 2 nd order periodic signal generator.	47
3.6	Comparison of magnitude frequency response of 1 st , 2 nd and 3 rd order periodic signal generators.	47
3.7	Block diagram of generic close-loop control system along with the plug-in repet- itive controller.	48
3.8	Internal structure of higher order plug-in repetitive controller.	48
3.9	Frequency response of 2 nd order odd harmonic periodic signal generator tuned at 50 Hz.	52
4.1	Block diagram of two level converter with conventional controller.	58
4.2	Frequency response of converter transfer function. The gain margin is 19.1 dB, the phase margin is 81.2 degrees and system bandwidth is 398 Hz.	60
4.3	Frequency response of converter transfer function along with proportional con- troller. The gain margin is 7.11, the phase margin is 52.9 degrees and system bandwidth is 1.62 KHz.	61

4.4	Output current of the converter controlled by PID. The grid voltage is as of case I and the current THD is 2.74%.	61
4.5	Output current of the converter controlled by PID. The grid voltage is as of case II and the current THD is 10.38%.	62
4.6	Block diagram of two level converter with repetitive controller.	62
4.7	Internal structure of odd harmonic repetitive controller used for the two level converter.	63
4.8	Pole zero map for the converter transfer function. The zero outside the unit circle indicates that the system is non-minimum.	63
4.9	Pole zero map for $T_d(z)$	64
4.10	Frequency phase plot of $T_d(z)z^m$ for various values of m	65
4.11	Frequency magnitude plot of K_u . The minimum value of K_u is 1.2.	65
4.12	Frequency response of two level converter along with the designed conventional odd harmonic repetitive controller. The gain margin is 9.14 dB. The phase margin is 46 degrees.	66
4.13	Frequency response of the disturbance transfer function. System bandwidth is about 1 KHz.	67
4.14	Converter output current for case II grid voltage. The THD is just 0.23%. Thus, repetitive controller successfully rejects odd harmonics in the grid.	67
4.15	Converter output current for case II grid voltage in the presence of 1% variation in grid frequency. The THD is 10.56%. Thus, repetitive controller fails to reject odd harmonics in the grid under frequency variation.	68
4.16	Frequency phase plot of $T_d(z)z^m$ for various values of m	70
4.17	Frequency magnitude plot of K_u . The minimum value of K_u is 1.	70
4.18	Frequency magnitude plot of converter along with the 2^{nd} order repetitive controller for different values of K_r	71
4.19	Frequency response of two level converter alongwith the designed 2^{nd} odd harmonic repetitive controller. The gain margin is -2.13 dB. The phase margin is 6.01 degrees.	72

4.20	Frequency response of the disturbance transfer function. System bandwidth is about 60 Hz.	72
4.21	Frequency response of two level converter along with the designed 2^{nd} order odd harmonic repetitive controller with the modified compensator. The gain margin is 3.67 dB. The phase margin is 27.1 degrees.	73
4.22	Frequency response of the disturbance transfer function. System bandwidth is about 230 Hz.	74
4.23	Converter output current for case II grid voltage in the presence of 1% variation in grid frequency. The controller is 2^{nd} order odd harmonic repetitive controller with the compensator given by (4.11). The current THD is 2.18%.	74
A.1	Block diagram of generic close loop control system.	78
A.2	Block diagram of generic close loop control system along with the plug-in repetitive controller.	81
A.3	Internal structure of plug-in repetitive controller.	82
A.4	Block diagram of generic close loop control system along with the plug-in higher order repetitive controller.	88
A.5	Internal structure of higher order plug-in repetitive controller.	88
B.1	Block diagram of close-loop system.	94

List of Tables

1	List of symbols used in this thesis.	13
4.1	Comparison of converter used in this work with other converters.	55
4.2	Harmonic currents limits according to ANSI/IEEE standard 519-1992.	56
4.3	Two cases for grid voltage harmonics. The first case was measured at a test site in Exeter University, U.K.	57
4.4	System parameters and component values for the two level grid connected con- verter with LCL filter.	59
4.5	Comparison of output current THD for different controllers.	75

Table 1: List of symbols used in this thesis.

No.	Symbol	Description
1	s	Frequency variable for Laplace transform
2	z	Z transform variable
3	$U(s)$	Control input/ Input of plant
4	$V(s)$	Disturbance signal
5	$R(s)$	Reference signal
6	$Y(s)$	Plant output
7	$G_c(s)$	Transfer function of controller
8	$G_p(s)$	Transfer function of plant
9	$T(s)$	Open loop gain
10	$H(s)$	Feedback transfer function
11	$E(s)$	Error signal
12	$P_o(s)$	Open loop characteristic polynomial
13	$D_r(s)$	Denominator of the Laplace transform of reference signal
14	$e(t)$	Error signal in time domain
15	K_p	Gain of proportional controller
16	T_p	Fundamental time period of periodic signal
17	$G_{im}(s)$	Transfer function of periodic signal generator
18	T_s	Sampling frequency. Its value is 50e-6 sec. unless specified otherwise.
19	N	Number of samples per period
20	$G_{RC}(z)$	Transfer function of repetitive controller

21	$Q(z)$	Transfer function of lowpass filter in repetitive controller
22	$G_x(z)$	Transfer function of stabilising compensator in repetitive controller
23	ω_n	Natural frequency of system (rad/s).
24	ζ	Damping ratio of system
25	f_s	Sampling frequency
26	$\ \cdot\ _\infty$	Infinity norm operator
27	T_{cl}	Close loop transfer function
28	K_r	Repetitive controller compensator gain
29	m	Number of lead steps
30	ω	Continuous-time frequency (rad/s)
31	Ω	Discrete-time frequency (rad)
32	ω_N	Nyquist frequency (rad/s)
33	$ \cdot $	Absolute value operator
34	$G_{oim}(z)$	Odd harmonic periodic signal generator
35	$G_{ho}(z)$	Higher order periodic signal generator
36	$W(z)$	Delay function of higher order periodic signal generator
37	$G_{HORC}(z)$	Transfer function of higher order repetitive controller
38	w_l	Weight of the l^{th} memory loop of higher order generator
39	$G_D(z)$	Transfer function from disturbance to output
40	$G_{horc}(z)$	Transfer function of higher order repetitive controller

Chapter 1

Motivation, Objectives and Contributions

1.1 Motivation

This research is motivated by the fact that the conventional repetitive controller fails to perform when the the frequency of the reference signal or disturbance signal changes from its known value[1].

The repetitive controller is a very useful technique for perfect tracking of periodic signals and disturbance rejection in systems which are afflicted by periodic disturbances. Grid connected converters, active filters used for power factor correction and multilink robotic manipulators are examples of those systems in which either the reference is periodic or the disturbances are periodic. All these systems are central to their respective industries. Thus, it is very important that these systems give desired performance. As it will be discussed later, repetitive controller has the ability to improve their performance considerably. Therefore, it is worth the time and effort to investigate the failure of repetitive controller under variations in known frequency.

The performance of a control loop depends on the gain of that loop. Repetitive controller substantially enhances the loop gain at the desired frequency and its harmonics. As any periodic signal is a sum of sinusoids of fundamental frequency and its harmonics, therefore, repetitive controller can provide large loop gain for any periodic signal. Figure 1.1 shows the magnitude frequency response of periodic signal generator which is a part of the repetitive controller. This periodic signal generator is tuned for 50 Hz and its harmonics. It can be seen that the

repetitive controller offers very large gains at the tuned frequency and its harmonics. Thus, by including the repetitive controller tuned at 50 Hz in a loop, the performance of that loop in terms of reference tracking and disturbance rejection can be enhanced. However, the problem

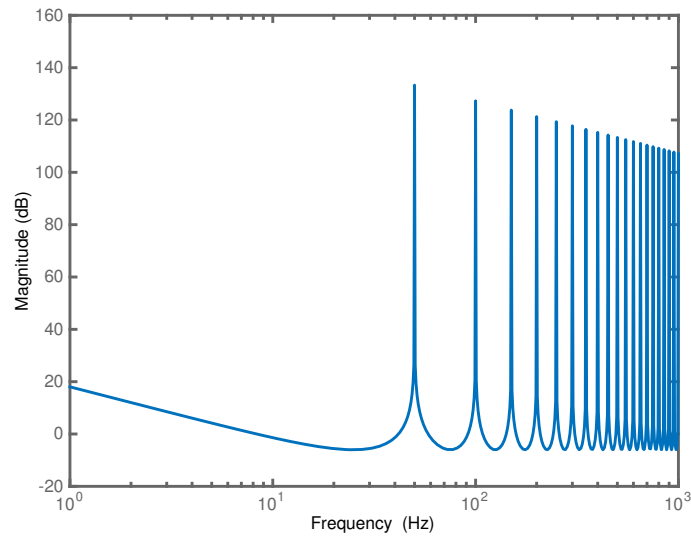


Figure 1.1: Frequency response of the discrete periodic signal generator tuned at 50 Hz.

is that the repetitive controller offers little gain in the neighbourhood of tuned frequency. This is apparent from figure 1.2. Therefore, if the frequency of the reference or disturbance signal changes from the predetermined value, the repetitive controller fails to offer adequate gain necessary for tracking/rejection. Thus, it fails to fulfil the purpose for which it is used in the first place.

One of the objective of this work is to provide a feasible solution for this problem.

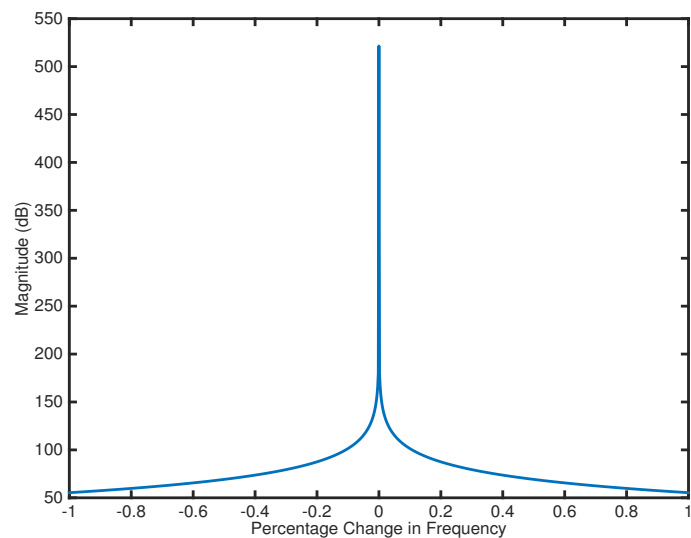


Figure 1.2: Magnitude frequency response of periodic signal generator in the neighbourhood of tuned frequency (50 Hz).

1.2 Aims and Objectives

This thesis aims to achieve following objectives.

1. Detailed introduction and analysis of conventional repetitive controller.
2. Analysis of performance degradation of conventional repetitive controller under variation in frequency of reference/disturbance.
3. Finding a solution for the problem of performance degradation under frequency variation.
4. Application of the conventional repetitive controller and the proposed solution to two level grid connected converter as a case study.

1.3 Contributions of Thesis

Following are the contributions of this thesis.

1. A detailed study of the conventional repetitive controller is carried out. All the related stability conditions are derived and presented in detail. Knowledge developed by this study is applied to the control of two level grid connected converter resulting in following publications.
 - Mohsin Jamil, **Usman Rashid**, Rizwan Arshad, Muhammad Nasir Khan, Syed Omer Gilani and Yasar Ayaz, “Robust repetitive current control of two level utility connected converter using LCL filter”, *Arabian Journal for Science and Engineering*, pp. 1-18, 2015.
 - Mohsin Jamil, Rizwan Arshad, **Usman Rashid**, Yasar Ayaz and Muhammad Nasir Khan, “Design and analysis of repetitive controllers for grid connected inverter considering plant bandwidth for interfacing renewable energy sources”, In *ICRERA, Milwaukee, USA*, 2014.
2. Various techniques for making the repetitive controller robust to frequency variation are explored. The robust high order repetitive controller is presented in detail. The related stability conditions and design procedures are also discussed.

3. The concept of phase lead compensation is extended to the design of robust high order repetitive controller.
4. The proposed scheme is applied to the control of two level grid connected converter. It is shown that the proposed controller's performance remains within desired limits under frequency variation.

1.4 Organisation of Thesis

The rest of the thesis is organised as follows:

In chapter 2, the conventional repetitive controller is discussed in detail. Starting from 1981, the history and developments in repetitive control are traced to the present day. Stability conditions are stated and derived in appendices. In the last section, the performance of repetitive controller under frequency variation is analysed.

Chapter 3 discusses various options for making the repetitive controller robust to frequency variations. Also, the theory of phase lead compensation is applied to high order repetitive controller.

In chapter 4, PID, conventional and high order repetitive controllers are applied for the current control of two level converter. It is shown by simulations that the conventional repetitive controller fails under frequency variation and the higher order repetitive controller successfully reject disturbances with varying frequency.

Chapter 5 concludes the thesis and gives recommendations for future work.

Chapter 2

Introduction to Repetitive Control

2.1 Synopsis

This chapter presents a brief introduction to the repetitive control theory. It starts from the basics of close loop feedback control system. The internal model principle is presented in a simple form. The proportional resonant controller is also discussed briefly.

The repetitive controller is introduced in the simplest possible terminology. The motivation behind its each component is explained in detail. Finally, the stability conditions for repetitive controller are presented. These derivations are detailed and use simple notation.

2.2 Performance of Close Loop System

A block diagram of generic close loop system is given in figure 2.1. The loop gain, i.e. $T(s)$, is given by following expression.

$$T(s) = G_c(s) \times G_p(s) \times H(s) \quad (2.1)$$

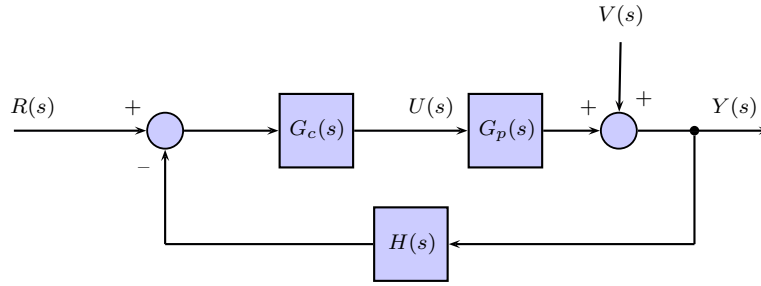


Figure 2.1: Block diagram of generic close loop control system.

2.2.1 Disturbance Rejection

The error in the system¹ is given by following equation.

$$E(s) = \frac{R(s)}{1 + T(s)} - \frac{H(s) \times V(s)}{1 + T(s)} \quad (2.2)$$

It is clear from this equation that the error in the system approaches zero as loop gain approaches infinity. Thus, by increasing loop gain, disturbances can be rejected.

2.2.2 Reference Tracking

The output of the system with respect to reference is given by the following transfer function.

$$Y(s) = \frac{G_c(s) \times G_p(s)}{1 + T(s)} \times R(s) \quad (2.3)$$

If the loop gain is high enough, $Y(s)$ becomes:

$$Y(s) = \frac{G_c(s) \times G_p(s)}{T(s)} \times R(s) = \frac{1}{H(s)} \times R(s) \quad (2.4)$$

The above equation shows that perfect reference tracking can be achieved by making the loop gain infinitely large and $H(s)$ close to unity.

Usually $H(s)$ is taken as unity. Also, the transfer function of plant, i.e. $G_p(s)$ cannot be modified. Thus, the loop gain can only be increased by appropriately designing the controller, i.e. $G_c(s)$. Hence, the controller should be designed in such a way that it has large gain value at those frequencies which need to be tracked or rejected.

¹The derivation of error equation is given in appendix A.1.

2.3 Internal Model Principle

The internal model principle (IMP) was proposed and proved by Francis and Wonham in 1976[2]. This principle relates the close loop performance of control system to applied reference and exogenous² disturbances. This principle can be understood easily³ in terms of open-loop characteristic polynomial (OLCP) of the system⁴ in figure 2.1. The OLCP expressed in terms of denominator of $G_c(s)$ and $G_p(s)$ is given by:

$$OLCP = P_o(s) = D_c(s)D_p(s) \quad (2.5)$$

Where

$$R(s) = \frac{N_r(s)}{D_r(s)} \quad (2.6)$$

$$G_c(s) = \frac{N_c(s)}{D_c(s)} \quad (2.7)$$

$$G_p(s) = \frac{N_p(s)}{D_p(s)} \quad (2.8)$$

Using this terminology, following theorem states the internal model principle.

Theorem 1 *In the configuration depicted in figure 2.1, where the poles of $R(s)$ are in the right half plane,*

$$\lim_{t \rightarrow \infty} e(t) = 0$$

if and only if

1. *The roots of the close loop system are in the left half plane.*
2. *$D_r(s)$ is a factor of the open-loop characteristic polynomial $P_o(s)$.*

This theorem simply states that the system in figure 2.1 can achieve perfect asymptotic⁵ reference tracking if it is stable and the denominator of $R(s)$ is a factor of $P_o(s)$. For example, a step reference can be tracked perfectly, i.e. with zero steady state error, by using an integrator as the controller⁶.

²Of, relating to, or developing from external factors.

³This explanation is based on a handout made by Prof. Stanislaw H. Zak. Available at: https://engineering.purdue.edu/~zak/ECE_382/hand_3.pdf

⁴Here the feedback gain, $H(s)$, is taken as unity.

⁵Asymptotic tracking means that the error of system eventually becomes zero over a long period of time.

⁶A complete description of this example can be seen in the handout mentioned in footnote no. 3.

It was mentioned in the previous section that the loop gain of the system should be increased for those frequencies which need to be tracked or rejected. The internal model principle is saying the same thing, but with much more mathematical rigour. Including the denominator of reference in the system's OLCP, actually increases the gain of the system at those frequencies which are part of the reference. Same is also true for the disturbance.

2.4 Proportional Resonant Controller

Proportional resonant controller (PRC) exploits the internal model principle to provide perfect reference tracking and disturbance rejection for the case of sinusoidal references and disturbances. A general sinusoidal signal can be modelled by:

$$\frac{A \times s}{s^2 + \omega_o^2}$$

This sinusoid's magnitude is A and its frequency is ω_o . The discussion in previous sections say that this kind of reference/disturbance can be tracked/rejected by increasing the loop gain, $T(s)$, at ω_o . In terms of internal model principle, model of sinusoid should be included in the controller. The proportional resonant controller does exactly the same thing. The structure of PRC is given by:

$$G_c(s) = K_p + \frac{K_r \times s}{s^2 + \omega_o^2} \quad (2.9)$$

As is clear from the above equation, PRC includes in itself the model of generic sinusoid signal. Thus, it has high gain at ω_o . This factor enables it to track and reject sinusoids having frequency ω_o . Figure 2.2 shows the response of a PRC tuned at 50 Hz. It can be seen that it has very large gain at the tuned frequency.

2.4.1 Limitations of Proportional Resonant Controller

The proportional resonant controller provides perfect tracking/rejection at the tuned frequency. However, it does not provide large gain at the harmonics of the tuned frequency which is usually required. For example, in electrical applications high loop gain is required at the fundamental for tracking and at its harmonics for rejection. This problem can be overcome by using a

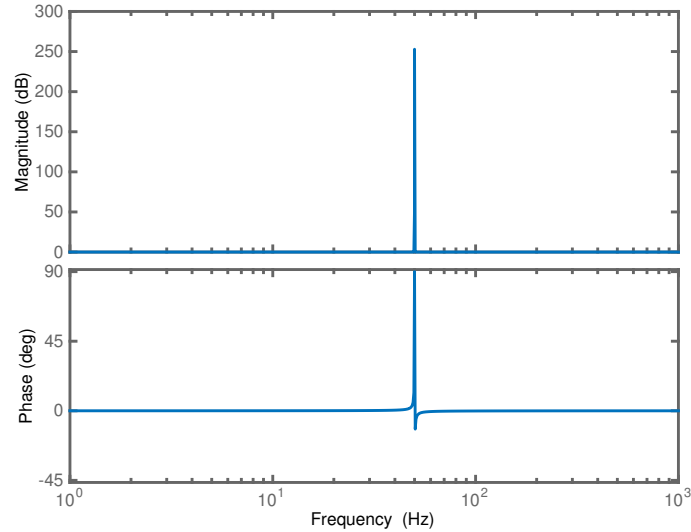


Figure 2.2: Frequency response of proportional resonant controller. This controller is tuned at 50 Hz and its both gains are unity.

number of PRCs in parallel which are tuned at the harmonic frequencies. This solution comes with its own baggage. With the inclusion of high frequency PRCs, the close loop stability of the system becomes a challenge. Also, the PRC suffers from frequency variation problem. Teodorescu et al. have discussed these problems thoroughly and have suggested solutions[3].

2.5 Repetitive Controller

Repetitive controller (RC) is a generalisation of proportional resonant controller. Where PRC provides high gain for a sinusoid reference with known period, RC does the same thing for any periodic signal with known period. RC achieves this by using a periodic signal generator. A periodic signal generator is a system which can generate any periodic signal of known period. According to internal model principle, perfect tracking is possible by including the generator of reference in the control loop. Thus, in theory, by including a periodic signal generator in the control loop, perfect tracking/rejection should be achieved for any desired periodic signal.

2.5.1 Periodic Signal Generator

Inoue et al. were the first to prove that a periodic signal generator can be used to track/reject a periodic signal with known period[4]. The structure of their generator is given in figure 2.3. The transfer function of this generator is given by following equation.

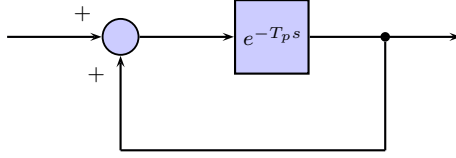


Figure 2.3: Structure of periodic signal generator.

$$G_{im}(s) = \frac{e^{-T_p s}}{1 - e^{-T_p s}} \quad (2.10)$$

where T_p is the period of the signal to be generated.

In order to generate a periodic signal from this model, the first period of the signal is provided as input. Then it keeps on generating the signal. It is able to generate the signal because of the presence of the lossless delay-line $e^{-T_p s}$. This delay-line delays the input signal for time T_p . This delayed signal appears on the output and is also fed back. This fed back signal is again delayed by one period and appears on the output after first cycle. The process of delay and feed back runs continuously, thus, generating the signal after the input has been removed.

Discrete Periodic Signal Generator

The periodic signal generator shown in figure 2.3 can not be realised physically as a precise and programmable delay-line⁷ can not be made. However, this generator has a counter part in discrete domain which can be implemented as a digital system. The discrete periodic signal generator⁸ is given by:

$$G_{im}(z) = \frac{z^{-N}}{1 - z^{-N}} \quad (2.11)$$

Where N is the number of samples per period.

$$N = \frac{T_p}{T_s} \quad (2.12)$$

T_s is the sampling time in discrete domain.

This periodic signal generator can be implemented by using N number of delay elements,

⁷A delay-line can be any material which delays the signal. The reader might have experienced a delay in voice over the telephone. This delay is caused in part by the copper wire which carries their voice.

⁸The derivation of discrete signal generator is given in appendix A.2.

i.e memory locations or registers, in a digital system. Figure 2.4 shows the generation of a periodic saw-tooth signal of 50 Hz. It can be seen that the signal was provided for only one cycle. The periodic signal generator produces rest of the cycles.

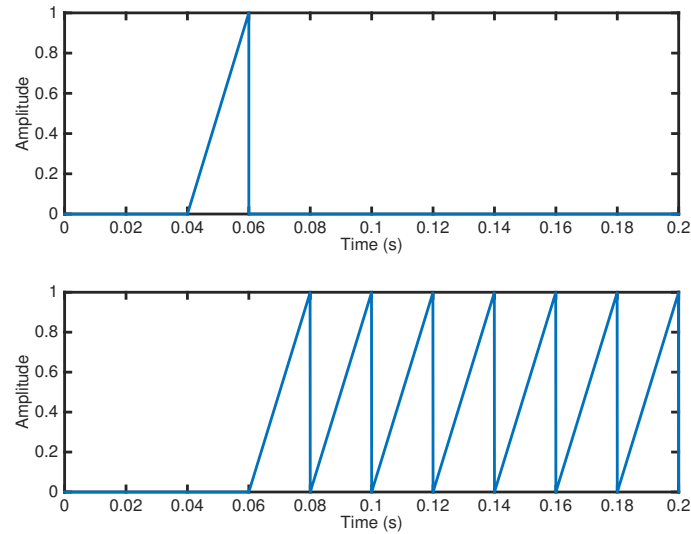


Figure 2.4: Signal generation by discrete periodic signal generator. The signal generated is of 50 Hz. The top plot is the input to periodic signal generator. The bottom plot is the output.

Frequency Intuition of Periodic Signal Generator

Periodic signal generator enables the repetitive controller to track/reject any periodic signal of known period. But, how? This question can be easily answered, once the theory of Fourier series is understood. According to Fourier series, every periodic signal can be expressed as a sum of sinusoids⁹. The Fourier series¹⁰ is given by:

$$f(t) = \frac{A_o}{2} + \sum_{n=1}^{\infty} A_n \sin\left(\frac{2\pi n t}{T_p} + \phi_n\right) \quad (2.13)$$

In the above expression, $f(t)$ is a periodic signal of known time period T_p . $\frac{A_o}{2}$ is the d.c. offset and A_n is the amplitude of n^{th} harmonic. This formula shows that every periodic signal is made up of sinusoids. The first sinusoid has the same time period T_p as that of the periodic signal. The rest of the sinusoids have time periods which are multiples of the fundamental period T_p .

Thus, a controller which can give very high gains at the fundamental frequency and its multiples for any periodic signal can perfectly track/reject that periodic signal. The repetitive

⁹A very intuitive graphical demonstration of Fourier series can be seen on wikipedia. Available at: http://en.wikipedia.org/wiki/Fourier_series

¹⁰The derivation of this form from commonly used form is given in appendix A.3.

controller has such capability because of the periodic signal generator. This point is demonstrated by considering the Fourier series of sawtooth signal shown in figure 2.4. Following equation gives the Fourier series of the saw-tooth signal¹¹.

$$f_{st}(t) = \frac{1}{2} - \sum_{n=1}^{\infty} \frac{1}{n\pi} \sin(2\pi 50nt) \quad (2.14)$$

This formula asserts that the saw-tooth signal whose frequency is 50 Hz is made up of a d.c offset and an infinite number of sine waves of frequency 50 Hz and its integer multiples. This is shown graphically in figure 2.5. On the other hand, the frequency response of discrete periodic

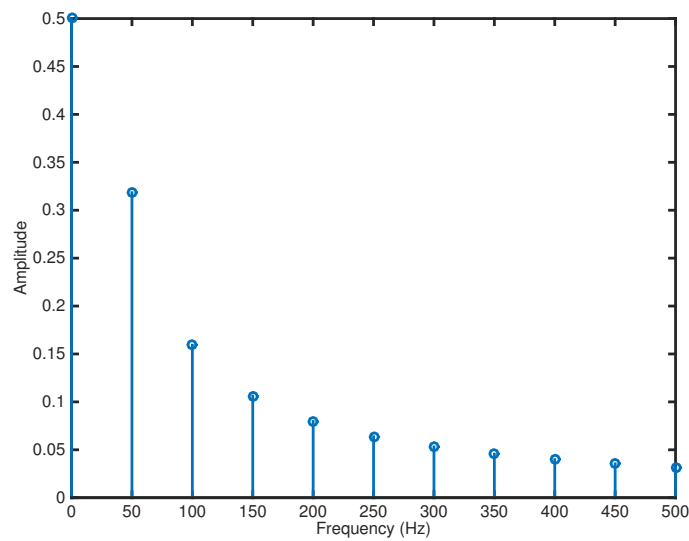


Figure 2.5: Magnitude of the Fourier coefficients, i.e A_0 and A_n , of saw-tooth signal of 50 Hz.

signal generator tuned at 50 Hz is shown in figure 2.6. The comparison of these two figures show that the periodic signal generator offers very high gains at fundamental frequency of saw-tooth signal and at its harmonics. Thus, by including this generator in the control loop, saw-tooth reference or disturbance of 50 Hz can be tracked/rejected perfectly.

2.5.2 Structure of Repetitive Controller

Repetitive controller includes the above discussed periodic signal generator as internal model. As the signal generator can only be implemented in discrete domain, thus, repetitive controller also can only be implemented in discrete domain.

It has been shown in the previous section that the signal generator gives very high gains at

¹¹Weisstein, Eric W. “Fourier Series–Sawtooth Wave.” From MathWorld–A Wolfram Web Resource. Available at: <http://mathworld.wolfram.com/FourierSeriesSawtoothWave.html>

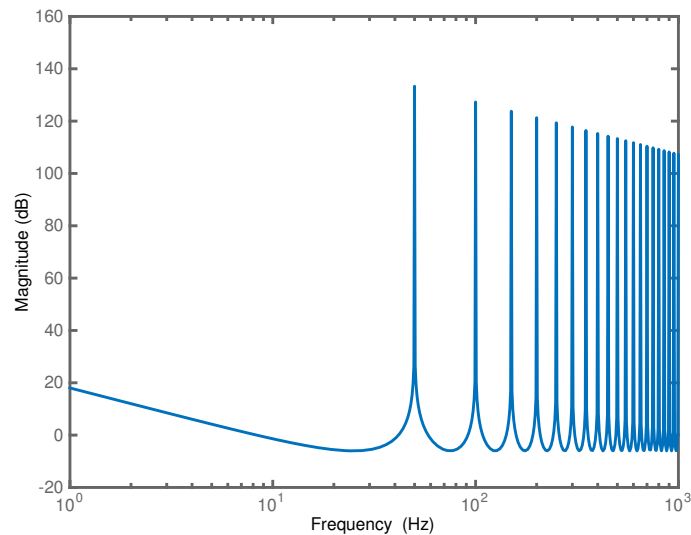


Figure 2.6: Frequency response of the discrete periodic signal generator tuned at 50 Hz.

the tuned frequency and its multiples upto infinity. This ability of the signal generator makes the stability of the close loop system very difficult to achieve. A number of repetitive control structures along with design algorithms have been introduced in the literature. The following section presents plug-in structure which was introduced by the inventors of repetitive control and has been used widely ever since.

Plug-in Repetitive Controller

In 1981, Inoue et al. published two papers[4][5], detailing the application of repetitive control to servomechanism and magnet power supply. However, they did not present a design algorithm at that time. In 1985, Hara et al. proposed[6] a structure for repetitive controller along with a design algorithm. They also presented sufficient¹² conditions for the stability of close loop system. In another work[7], Hara et al. generalised their design algorithm and stability conditions to multi input multi output (MIMO) systems.

In 1990, Inoue presented[8] the structure, design algorithm and stability conditions for the repetitive controller that they had used for the applications presented in their earlier papers. Inoue cited Hara et al. and also used their arguments to support his own conclusions. The structure of repetitive controller proposed by Inoue et al. and Hara et al. is known as plug-in repetitive controller. Tsai and Yao further developed this structure[9]. This structure is known as plug-in because of the fact that the repetitive controller is plugged into a stable close loop

¹²If P is a sufficient condition for Q, then $P \rightarrow Q$. This means that if P is true, then Q is also true. However, if Q is true, P can be true or false.

system. The control loop is first made stable using conventional control algorithms such as PID or pole placement method; then, the repetitive controller is plugged in the loop. Before plugging in, the repetitive controller is modified in such a way that it does not destabilise the system. Figure 2.7 shows a generic close loop control system along with a plug-in repetitive controller[9]. The internal structure of the repetitive controller is shown in figure 2.8.

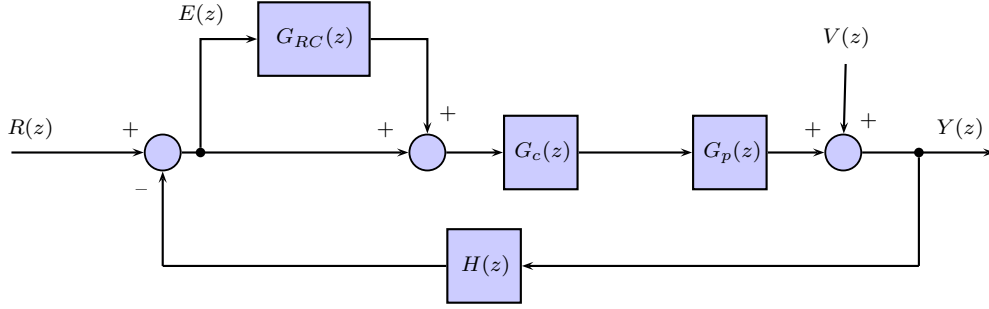


Figure 2.7: Block diagram of generic close loop control system along with the plug-in repetitive controller.

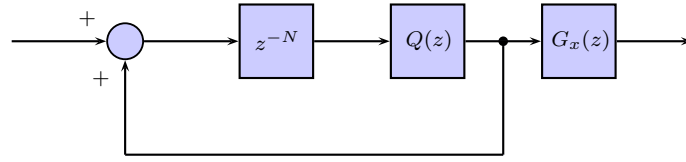


Figure 2.8: Internal structure of plug-in repetitive controller.

The repetitive controller contains two additional components along with the periodic signal generator. These components are: (i) a lowpass filter $Q(z)$ and (ii) a stabilising compensator $G_x(z)$.

Motivation behind $Q(z)$ and $G_x(z)$

It has been shown in previous sections that the periodic signal generator provides very high gains at the tuned frequency and its harmonics. It was shown that this property is of great benefit as it provides asymptotic tracking and disturbance rejection. However, this property has a side effect. The side effect is demonstrated by taking the example of following 3rd order plant.

$$G_p(s) = \frac{K \times w_n^2}{s(s^2 + 2\zeta w_n s + w_n^2)} \quad (2.15)$$

This plant has following parameters:

$$K = 1000$$

$$w_n = 2 \times \pi \times 1000$$

$$\zeta = 0.7$$

The frequency response of this plant is shown in figure 2.9. It is clear from the frequency response that this plant has large gain margin and phase margin. It has large D.C. gain. In other words, this plant does not require any control to behave properly. It can be connected in close loop without any controller and it will give ‘desired’ performance. In order to track

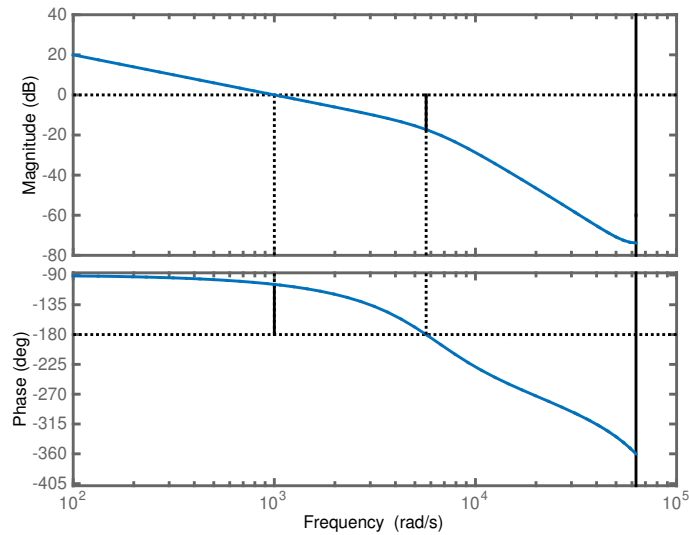


Figure 2.9: Frequency response of a test 3rd order plant. The gain margin is 17.3 and phase margin is 75.7.

sinusoidal reference of 50 Hz, a periodic signal generator tuned at 50 Hz is added to the loop. The frequency response of the resulting system is shown in figure 2.10. It can be seen in the figure that the system has very small gain margin and phase margin. And both the margins are negative. This example shows that the direct inclusion of periodic signal generator in the loop substantially degrades the stability margins. Even if the system remains stable, it has very tight stability conditions which are easily violated by parameter changes in actual plant. Thus, making the loop unstable. It is, therefore, necessary to modify the periodic signal generator in such a way so that it does not degrade the stability margins of the system to which it is added. For this purpose, $Q(z)$ and $G_x(z)$ are used.

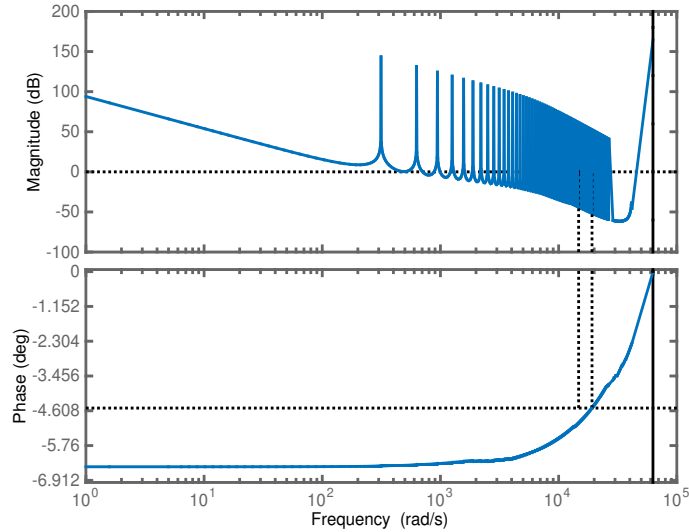


Figure 2.10: Frequency response of the test 3^{rd} order plant with periodic signal generator added. The gain margin is -0.276 and phase margin is -0.428 .

Lowpass Filter $Q(z)$

The lowpass filter $Q(z)$ is used to shape the response of periodic signal generator. The generator provides high gain at harmonic multiples upto infinity. The gain at high order harmonic multiples make the stability of repetitive controller a challenge. Hara et al. proved that the stability conditions for repetitive control system can be relaxed by using a lowpass filter in series with periodic signal generator[7]. This relaxation in stability conditions come at a price. The lowpass filter attenuates the gain of periodic signal generator at high frequencies. Thus, the signals; saw-tooth, square, etc.; which contain sharp edges cannot be tracked perfectly as the loop containing the modified periodic signal generator does not provide gain at high frequencies. Of course, the cut-off frequency of the lowpass filter can be selected to include desired frequency components. But, again this increase makes the loop more difficult to stabilise. Figure 2.11 shows the response of modified periodic signal generator. It is evident that the lowpass filter has considerably attenuated its gain at high frequencies.

A lowpass filter which has been widely used in literature is a moving average non-causal¹³ first order filter. It is given by following equation.

$$Q(z) = 0.25z + 0.5 + 0.25z^{-1} \quad (2.16)$$

A non-causal filter cannot be implemented independently as it depends on future inputs. How-

¹³A system whose output depends on future input.

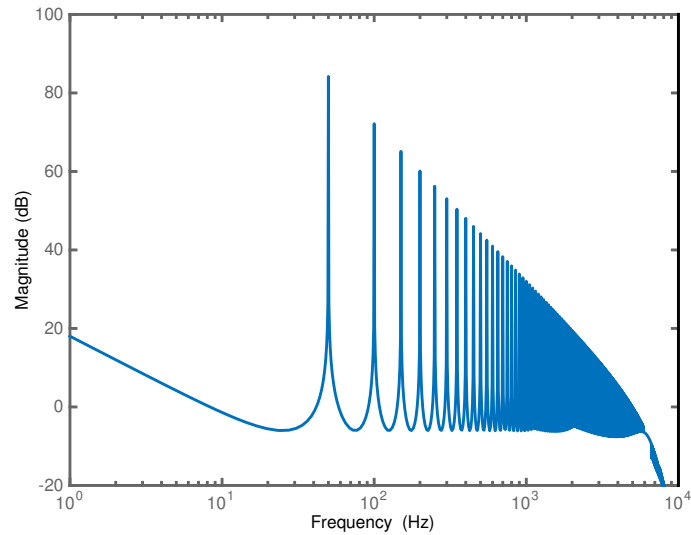


Figure 2.11: Frequency response of periodic signal generator with lowpass filter added.

ever, it can be implemented in series with the delay element z^{-N} . The frequency response of this filter is shown in figure 2.12. This filter has zero phase which means that it does not disturb the phase of overall loop. Also it has large enough bandwidth. For $f_s = 20$ KHz, its bandwidth is about 3.6 KHz, which means that the periodic signal generator in which it is added can provide good tracking/rejection for signals upto 3.6 KHz.

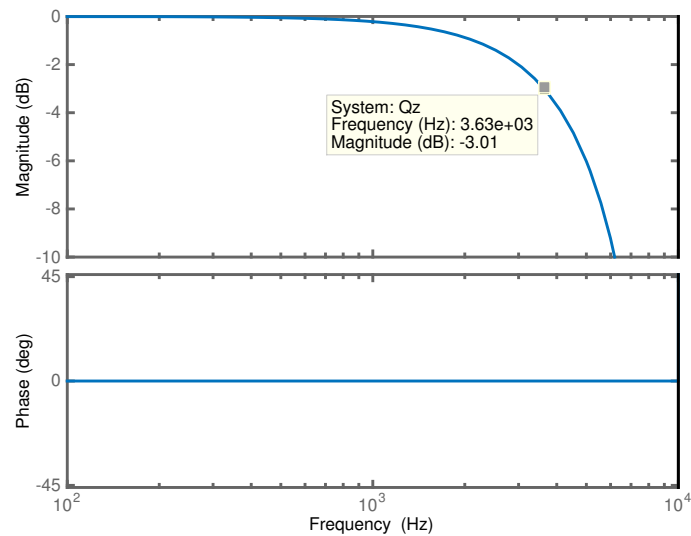


Figure 2.12: Frequency response of lowpass filter.

2.5.3 Stability Analysis of Repetitive Control System

In order to understand the purpose and design of stabilising compensator, it is necessary that the stability of repetitive control system be analysed. Two methods have been used in liter-

ature for the stability analysis of repetitive control system, i.e. the small gain theorem¹⁴ and regeneration spectrum[10]. Small gain theorem is much simpler and results in very intuitive stability conditions as compared to regeneration spectrum.

Analysis by Small Gain Theorem

The sensitivity function of the repetitive control system shown in figure 2.7 is given by:

$$\frac{Y(z)}{V(z)} = \frac{1}{1 + T(z)} \quad (2.17)$$

Where

$$T(z) = (1 + G_{RC}(z))G_c(z)G_p(z) \quad (2.18)$$

Here $H(z)$ is taken as unity. According to small gain theorem, the system is input output stable (IOS) if:

$$\|T(z)\|_\infty < 1 \quad (2.19)$$

However, the above condition does not give much insight into the system. Following the reasoning in [11], equation (2.18) is simplified¹⁵ as follows.

$$\frac{Y(z)}{V(z)} = (1 - z^{-N}Q(z)) \times \frac{1}{1 + G_c(z)G_p(z)} \times \frac{1}{1 + (T_{cl}(z)G_x(z) - 1)z^{-N}Q(z)} \quad (2.20)$$

Where

$$T_{cl}(z) = \frac{G_c(z)G_p(z)}{1 + G_c(z)G_p(z)} \quad (2.21)$$

Now in order to prove the stability of repetitive control system, the stability of the three subsystems in equation (2.20) need to be proved. This is done by considering each system turn by turn.

1. $1 - z^{-N}Q(z)$ is stable as $Q(z)$ is a stable lowpass filter. Also, $\|1 - z^{-N}Q(z)\|_\infty < \infty$. Thus, this system is H_∞ stable.
2. $\frac{1}{1 + G_c(z)G_p(z)}$ is stable as $G_c(z)$ is designed in such a way that the close loop system without repetitive controller is stable with large margins.

¹⁴A detailed discussion on small gain theorem is present in appendix B.1.

¹⁵Stepwise simplification is present in appendix A.4.

3. $\frac{1}{1+(T_{cl}(z)G_x(z)-1)z^{-N}Q(z)}$ determines the stability of the repetitive control system. The small gain theorem says that this system is stable if $\|(T_{cl}(z)G_x(z) - 1)z^{-N}Q(z)\|_\infty < 1$. Using the triangular inequality, this condition is modified to $\|(T_{cl}(z)G_x(z) - 1)z^{-N}Q(z)\|_\infty \leq \|T_{cl}(z)G_x(z) - 1\|_\infty \|Q(z)\|_\infty \|z^{-N}\|_\infty < 1$. As $\|z^{-N}\|_\infty = 1$, thus, the stability condition becomes $\|T_{cl}(z)G_x(z) - 1\|_\infty < 1$ and $\|Q(z)\|_\infty \leq 1$.

The above discussion is summarised by the following theorem.

Theorem 2 *The repetitive control system shown in figure 2.7 is stable if¹⁶*

1. $\|Q(z)\|_\infty \leq 1$ ¹⁷
2. $T_{cl}(z)$ is stable.
3. $\|T_{cl}(z)G_x(z) - 1\|_\infty < 1$.

2.5.4 Stabilising Compensator $G_x(z)$

Inverse Model Compensator

A natural choice for $G_x(z)$ is:

$$G_x(z) = \frac{K_r}{T_{cl}(z)} \quad (2.22)$$

Here K_r is constant gain which determines the amount of repetitive action in the loop. Its value can be selected by analysing the bode plot of the system. This compensator is a direct result of condition 3 in theorem 2. This compensator brings down the design of repetitive controller to the simple choice of gain K_r . However, there is a catch. This compensator requires the inverse of close loop transfer function, $T_{cl}(z)$. This inverse is stable only if $T_{cl}(z)$ is minimum phase system, i.e. all its zeros are within the unit circle. If $T_{cl}(z)$ is non-minimum phase then it has zeros outside the unit circle and its inverse has poles outside the unit circle.

Thus, this compensator cannot be used for non-minimum phase plants. Also, in the case of minimum phase plants, parameter changes can result in large deviation from the known transfer function. To overcome these problems, Zhang et al. proposed a phase lead compensation solution[12].

¹⁶This theorem gives a sufficient condition for stability. That is why ‘if’ is used instead of ‘if and only if’.

¹⁷This condition can be easily satisfied by choosing a lowpass filter which has 0 dB passband and less than 0 dB stopband gain. The filter given in (2.16) satisfies this condition.

Phase Lead Compensator

Phase lead compensator[12] is given by:

$$G_x(z) = K_r z^m \quad (2.23)$$

This compensator has two components. K_r is gain element which has zero phase and z^m is phase element which has unity gain. m is a positive integer. The frequency response of $G_x(z)$ is given by:

$$G_x(e^{j\Omega}) = e^{jm\Omega} \quad (2.24)$$

Where

$$\Omega = \omega T_s$$

Thus, the phase of $G_x(z)$ in radians is given by:

$$\theta_{G_x} = m\omega T_s \quad (2.25)$$

The phase in degrees is given by:

$$\theta_{G_x} = m\omega T_s \frac{180^\circ}{\pi} = m\omega \frac{180^\circ}{\omega_N} \quad (2.26)$$

Where ω_N is the Nyquist frequency which is equal to the half of sampling frequency. This equation shows that the lead compensator has linear phase which is zero at $\omega = 0$ and $180^\circ m$ at $\omega = \omega_N$. The frequency phase response of $G_x(z)$ is shown in figure 2.13. In order to understand how phase lead compensator stabilises the repetitive control system, the stability conditions in theorem 2 need further analysis. If condition 2 is satisfied, then the remaining two conditions can be rewritten together as:

$$\|(T_{cl}(z)G_x(z) - 1)Q(z)\|_\infty < 1 \quad (2.27)$$

Substituting $G_x(z)$ from equation (2.23) gives:

$$\|(T_{cl}(z)k_r z^m - 1)Q(z)\|_\infty < 1 \quad (2.28)$$

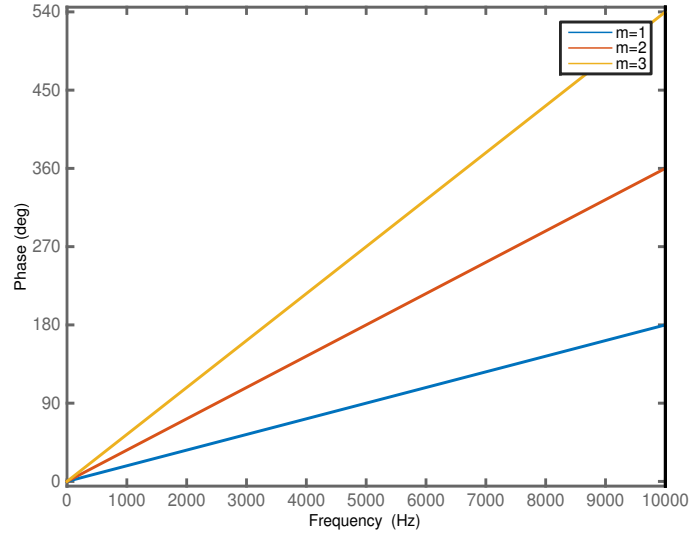


Figure 2.13: Frequency response of $G_x(z)$ for various values of m . Note that both axes have linear scales.

Representing this equation in frequency domain gives:

$$\|(M_{T_{cl}}(e^{j\Omega})e^{j\theta_{T_{cl}}(e^{j\Omega})}k_r e^{jm\Omega} - 1)M_Q(e^{j\Omega})e^{j\theta_Q(e^{j\Omega})}\|_{\infty} < 1 \quad (2.29)$$

Where $M(e^{j\Omega})$ is the magnitude response and $\theta(e^{j\Omega})$ is the phase response. Using the definition of infinity norm, equation (2.29) can be written as:

$$|(M_{T_{cl}}(e^{j\Omega})e^{j\theta_{T_{cl}}(e^{j\Omega})}k_r e^{jm\Omega} - 1)M_Q(e^{j\Omega})e^{j\theta_Q(e^{j\Omega})}| < 1 \text{ for } 0 < \Omega < \pi \quad (2.30)$$

Using the definition of absolute value, the above equation can be rearranged as:

$$|(1 - M_{T_{cl}}(e^{j\Omega})e^{j\theta_{T_{cl}}(e^{j\Omega})}k_r e^{jm\Omega})M_Q(e^{j\Omega})e^{j\theta_Q(e^{j\Omega})}| < 1 \text{ for } 0 < \Omega < \pi \quad (2.31)$$

Following the reasoning in [12] and [13], the above stability condition is simplified to following three stability conditions.¹⁸

$$0 < K_r < \frac{2\cos(m\Omega + \theta_{T_{cl}})}{M_{T_{cl}}} \text{ for } 0 < \Omega < \pi \quad (2.32)$$

$$0 \leq M_Q \leq 1 \text{ for } 0 < \Omega < \pi \quad (2.33)$$

¹⁸A detailed step by step derivation is given in appendix A.5.

Also, for K_r to be positive following condition must be satisfied.

$$|m\Omega + \theta_{T_{cl}}| < 90^\circ \text{ for } 0 < \Omega < \pi \quad (2.34)$$

Following theorem is formulated from these conditions.

Theorem 3 *The repetitive control system shown in figure 2.7 is stable for $G_x(z) = K_r z^m$ if,*

1. $\|Q(z)\|_\infty \leq 1$
2. $T_{cl}(z)$ is stable.
3. $0 < K_r < \frac{2\cos(\theta_{T_{cl}}(e^{j\Omega}) + m\Omega)}{M_{T_{cl}}(e^{j\Omega})}$ for $0 < \Omega < \pi$
4. $|\theta_{T_{cl}}(e^{j\Omega}) + m\Omega| < 90^\circ$ for $0 < \Omega < \pi$

It is clear from this theorem that the phase lead compensator can stabilise the repetitive control system as it adds positive phase $m\Omega$, thus, satisfying condition 4. After choosing m to satisfy condition 4, condition 3 can be satisfied by choosing appropriate value of K_r .

2.5.5 Odd Harmonic Periodic Signal Generator

The periodic signal generator discussed in section 2.5.1 gives high gain at all harmonics of the tuned frequency. However, in many applications only odd harmonics are present. Griñó et al. proposed a periodic signal generator which has high gains only at odd harmonics[11]. Their proposed signal generator is given by following equation.

$$G_{oim} = \frac{-z^{-\frac{N}{2}}}{1 + z^{-\frac{N}{2}}} \quad (2.35)$$

The structure of this internal model is shown in figure 2.14. Its frequency magnitude response is shown in figure 2.15. This figure shows that the internal model has high gain only at the tuned frequency and its odd harmonics. A big advantage of using this internal model is that its memory requirements are half ($\frac{N}{2}$) as compared to conventional periodic signal generator.

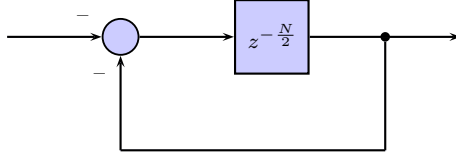


Figure 2.14: Structure of odd harmonic periodic signal generator.

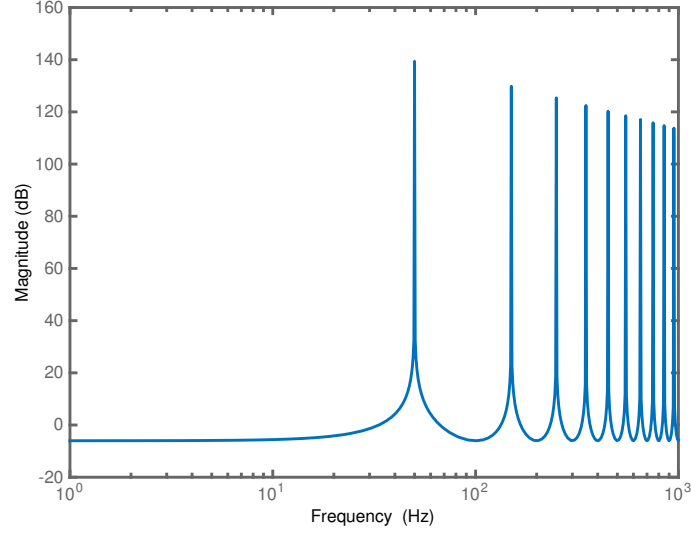


Figure 2.15: Frequency response of odd harmonic periodic signal generator.

Motivation behind Odd Harmonic Signal Generator

The odd harmonic periodic signal generator exploits the following property of odd harmonic periodic signals in discrete domain.

$$x\left(n + \frac{N}{2}\right) = -x(n) \quad (2.36)$$

Where N is the number of samples per period. It is given by following equation.

$$N = \frac{T_p}{T_s} \quad (2.37)$$

Figure 2.16 shows the first period of following odd harmonic periodic signal.

$$x(n) = \sin(2\pi 50nT_s) + \sin(2\pi 150nT_s) \quad (2.38)$$

The sampling time for this signal is 0.0002 seconds. Its fundamental period is 50 Hz. It contains only third harmonic. Thus, N for this signal is 100. From figure 2.16 it is evident that this

signal satisfies (2.35). An interesting consequence of (2.35) is that the odd harmonic periodic

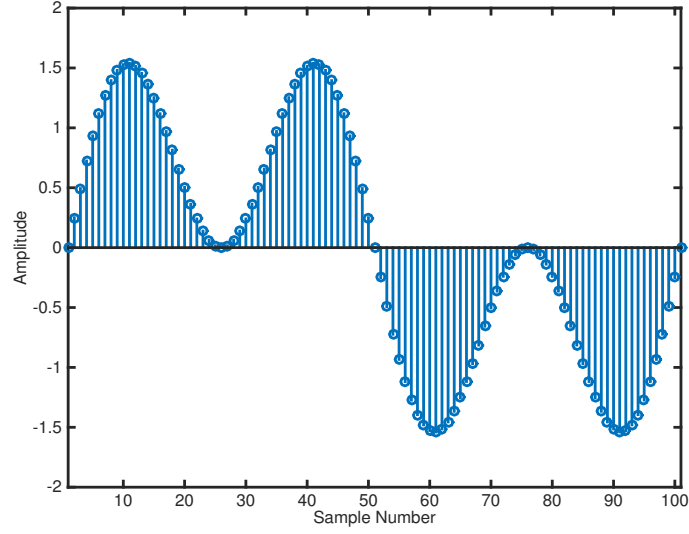


Figure 2.16: An odd harmonic signal having period 50 Hz.

signals can be constructed by adding delayed copies of their half period.

$$x(n) = \sum_{k=0}^{k=\infty} (-1)^k x_1(n - k \frac{N}{2}) \quad (2.39)$$

Where

$$x_1(n) = \begin{cases} x(n) & 0 \leq n \leq \frac{N}{2} - 1 \\ 0 & \text{elsewhere} \end{cases} \quad (2.40)$$

This is exactly what the odd harmonic periodic signal generator does. It delays the signal by half period and inverts its sign.

Structure of Odd Harmonic Repetitive Controller

Except the periodic signal generator, the structure of odd harmonic repetitive controller is same as that of conventional repetitive controller. Also, very interestingly, the stability conditions in theorem 2 and 3 also apply to odd harmonic repetitive controller[11][12].

2.6 Repetitive Controller under Frequency Variation

The performance of repetitive controller is known to be sensitive to variation in frequency of reference/disturbance. It has been discussed in previous sections that the periodic signal

generator used by the repetitive controller is tuned at a specific frequency. However, when the frequency of reference/disturbance varies, the periodic signal generator is unable to adapt to this change. Also, it offers considerably small gain in the neighbourhood of tuned frequency and its harmonics. This is true for both conventional and odd harmonic periodic signal generators.

Figure 2.17 shows the magnitude response of periodic signal generator in the neighbourhood of tuned frequency which is 50 Hz in this case. The red tickers are at 49, 50 and 51 Hz. It is evident that the periodic signal generator offers substantially small gain at 49 and 51 Hz. Thus, a small change of 1 Hz in the frequency of reference/disturbance can render the repetitive control system ineffective. Figure 2.18 shows the magnitude against the percentage change

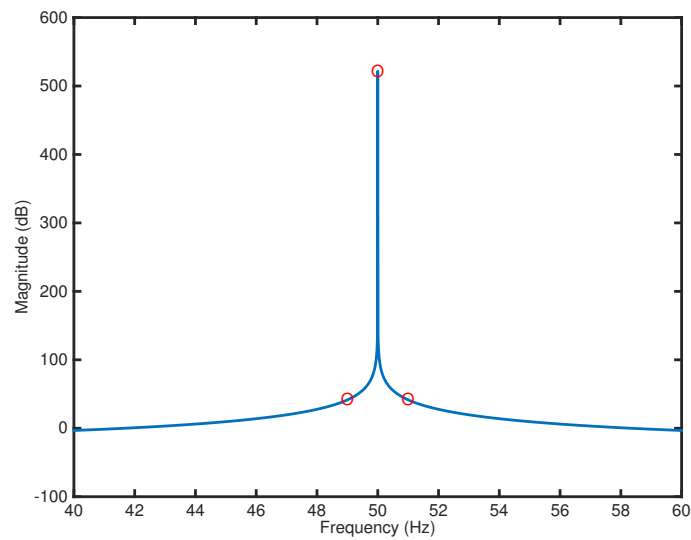


Figure 2.17: Magnitude frequency response of periodic signal generator in the neighbourhood of tuned frequency (50 Hz).

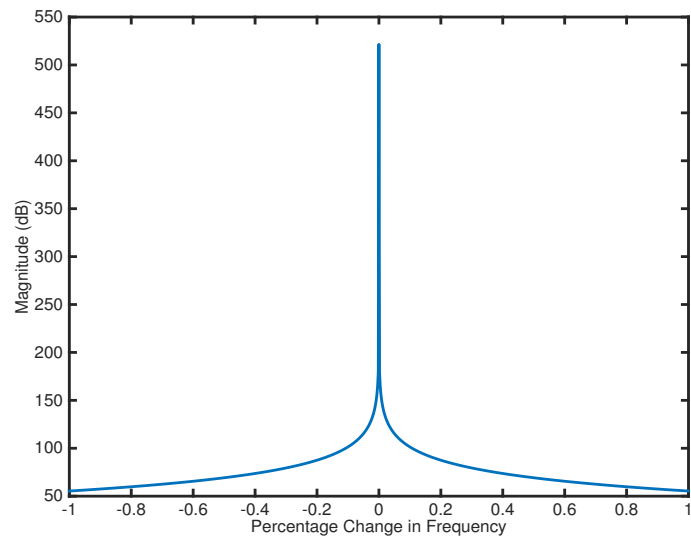


Figure 2.18: Magnitude frequency response of periodic signal generator in the neighbourhood of tuned frequency.

in frequency from tuned frequency. It can be seen that with one percent change in frequency the gain of periodic signal generator falls down to 50 dB. This demonstrates that the periodic signal generator is highly sensitive to changes in frequency.

As high gain is required for reference tracking and disturbance rejection, the repetitive control system fails to give desired tracking/rejection in the neighbourhood of tuned frequency. Therefore, in the presence of uncertainty in reference/disturbance frequency; the repetitive controller fails. The meaning and effects of this failure are different for each system. In chapter 4, the case of grid connected converter is discussed. There it is shown that the failure of conventional repetitive controller results in violation of international/national quality standards, which in turn, can incur physical/financial loss.

Chapter 3

Repetitive Controller Robust to Frequency Variation

3.1 Introduction

This chapter discusses in detail two solutions from literature which can be used to overcome the problem of performance degradation of repetitive controller under frequency variation. Ramos et al. have proposed that the tuned frequency of the repetitive controller can be changed by changing its sampling frequency[14]. It is a simple and intuitive solution. However, with the change in sampling frequency, the dynamics of the controlled plant change. This change can destabilise the system[15].

Steinbuch has proposed a higher order repetitive controller which has large gain in the neighbourhood of tuned frequency[16]. The problem with the higher order repetitive controller is that it improves the periodic performance at the cost of non-periodic performance[17]. However, it is possible to find a compromise between periodic and non-periodic performance as discussed in [17].

3.2 Frequency Adaptive Repetitive Controller

In order to overcome the problem of performance degradation of repetitive controller under frequency variation, Ramos et al. proposed a sampling period varying repetitive controller[14]. Their idea is very simple and intuitive: change the tuned frequency of the repetitive controller

with the change in reference/disturbance frequency. The tuned frequency for the digital repetitive controller is selected by evaluation of N which is given by following equation.

$$N = \frac{T_p}{T_s} \quad (3.1)$$

Where T_s is the sampling time and T_p is the time period of the periodic signal which is to be tracked or rejected. The corresponding repetitive controller is given by following equation.

$$G_{RC} = \frac{z^{-N}Q(z)G_x(z)}{1 - z^{-N}Q(z)} \quad (3.2)$$

This repetitive controller has high gains at $f_p = \frac{1}{T_p}$ Hz and its harmonics upto the cutoff frequency of the lowpass filter $Q(z)$.

If the time period of the tracked signal changes from T_p to \tilde{T}_p , the repetitive controller can adjust its frequency response by changing its sampling period. The sampling period for \tilde{T}_p is given by following equation.

$$\tilde{T}_s = \frac{\tilde{T}_p}{N} \quad (3.3)$$

This technique is implemented by using a phase lock loop (PLL) as shown in figure 3.1. The phase lock loop produces sampling frequency for the digital components of the repetitive control system. This sampling frequency is a multiple of the output frequency which is equal to the reference/disturbance frequency. In this way, the repetitive controller's tuned frequency remains in lock with the reference/disturbance frequency. Figure 3.2 shows the magnitude

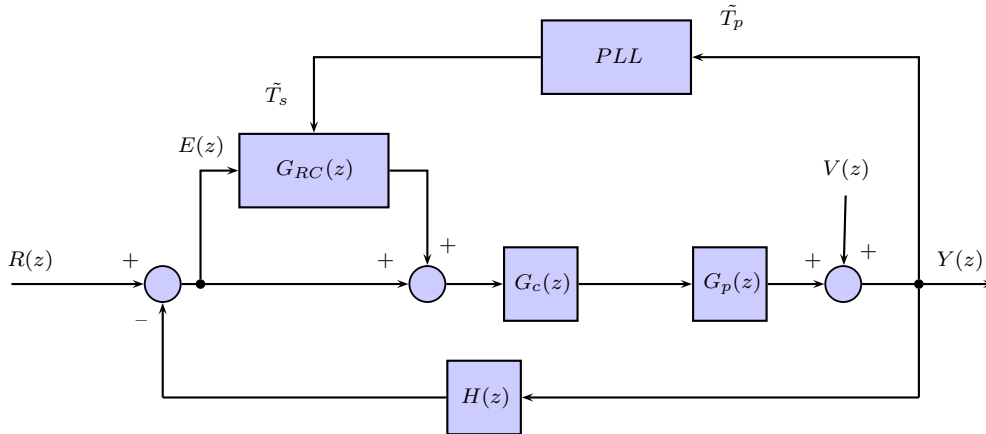


Figure 3.1: Block diagram of generic close-loop control system along with the frequency adaptive plug-in repetitive controller.

frequency response of a repetitive controller whose tuned frequency is changed from 50 Hz to 49 Hz and then to 51 Hz by changing its sampling frequency. The major advantage of this scheme is that the internal structure of repetitive controller remains same. Also, the number of memory elements, N , required for digital implementation of repetitive control remain same as the frequency variation is compensated by changing the sampling frequency of the repetitive controller and not N . In addition to the PLL, suitable hardware, i.e. Digital Signal Processor (DSP), Digital to Analog Converter (DAC) and Analog to Digital Converter (ADC), is required which can run on variable sampling frequency.

It must be ascertained that the repetitive control system does not become unstable by variation in sampling frequency. Ramos et al. derived stability conditions for frequency adaptive repetitive controller[18]. They also determined the range of sampling frequency for which the repetitive control system remains stable.

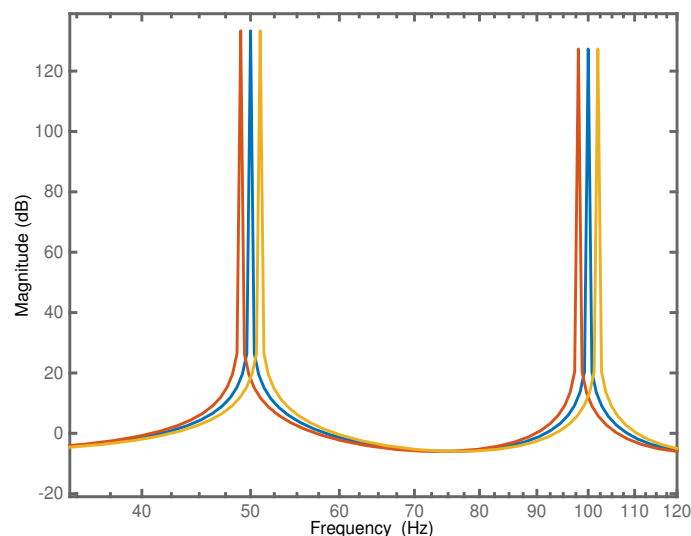


Figure 3.2: Frequency response of adaptive repetitive controller tuned at 50 Hz. As the frequency of reference/disturbance changes, its tuned frequency is shifted by changing its sampling frequency.

3.2.1 Difficulties in Implementing Adaptive Repetitive Controller

The major difficulty in implementing the adaptive repetitive controller is that the frequency of the output has to be estimated in real time very precisely. Without real time estimation, the sampling time of the repetitive control system cannot be updated. The error in the estimated frequency should be smaller than 0.2% in order for the adaptive repetitive controller to work properly. This is evident from figure 3.3 where it can be seen that for a difference of 0.2%

from the tuned frequency, the repetitive controller offers small gain. Also, the change in sam-

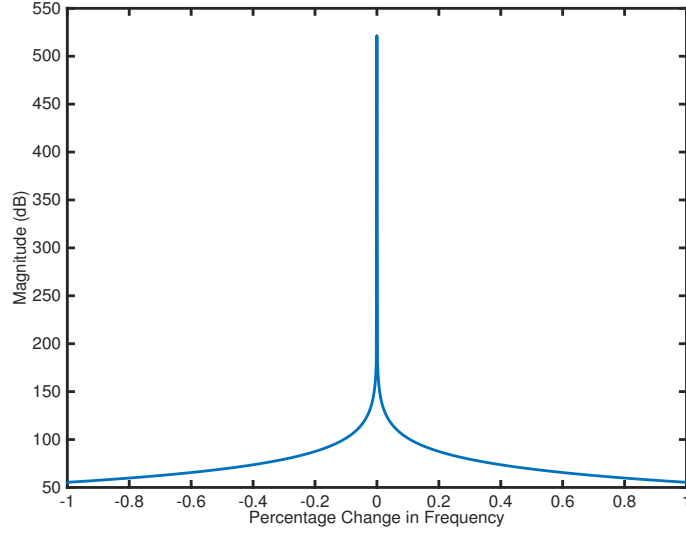


Figure 3.3: Magnitude frequency response of periodic signal generator in the neighbourhood of tuned frequency.

pling frequency changes the dynamics of the controlled plant. As the design of the stabilising compensator $G_x(z)$ is dependent on the plant, thus, it has to be robust so that the repetitive control system does not become unstable with the change in sampling period.

3.3 Higher Order Repetitive Controller

Steinbuch proposed higher order repetitive controller (HORC)[16] to solve the problem of performance degradation under frequency variation. The difference between a conventional and higher order repetitive controller is that of periodic signal generator. The periodic signal generator used by the higher order repetitive controller offers relatively high gains in the neighbourhood of tuned frequency and its harmonics. Similar to conventional repetitive control system, higher order repetitive control system requires a lowpass filter and a stabilising compensator for stable operation.

3.3.1 Higher Order Periodic Signal Generator

Instead of using one memory loop, higher order generator uses multiple weighted memory loops. Figure 3.4 shows the structure of third order periodic signal generator. A general higher order

periodic signal generator is given by following equations.

$$G_{ho} = \frac{W(z)}{1 - W(z)} \quad (3.4)$$

Where

$$W(z) = \sum_{l=1}^m w_l z^{-lN} \quad (3.5)$$

m is the order of this periodic signal generator. w_l is the weight of l^{th} memory loop. The frequency response of the higher order generator is highly dependent on these weights.

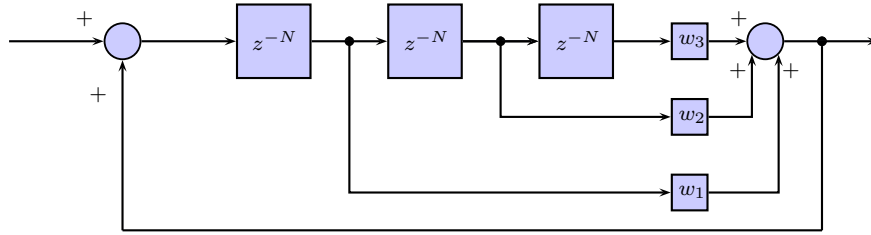


Figure 3.4: Structure of 3rd order periodic signal generator.

Calculation of Weights w_l

The method described in this section to calculate the weights follow the reasoning in [19]. The objective is to find such weights so that the higher order periodic signal generator gives infinite gain at the tuned frequency and its harmonics. This can be achieved by making the value of $W(z)$ equal to 1 and its first $m - 1$ derivatives equal to 0 at the tuned frequency and its harmonics. It is evident from (3.4) that $G_{ho}(z)$ has infinite gain when $W(z) = 1$. For the m^{th} order generator, the weights can be found by using following two formulae¹.

$$\sum_{l=1}^m w_l = 1 \quad (3.6)$$

And

$$\sum_{l=1}^m w_l l^p = 0 \text{ for } p = 1, 2, 3, \dots, m - 1 \quad (3.7)$$

¹A detailed derivation of these formulae is given in appendix A.6.

Using these formulae, the weights for 2^{nd} order periodic signal generator are evaluated².

$$w_1 = 2 \text{ and } w_2 = -1 \quad (3.8)$$

Similarly, the weights for 3^{rd} order generator are:

$$w_1 = 3, w_2 = -3 \text{ and } w_3 = 1 \quad (3.9)$$

Frequency Response

The magnitude frequency response of 2^{nd} order periodic signal generator is shown in figure 3.5. From this figure, the response of 2^{nd} order generator looks almost same as that of first order generator. Similar to first order periodic signal generator it has very high gain at the tuned frequency and its harmonics. However, the advantage of higher order generator becomes evident when its magnitude frequency response is compared with that of first order periodic signal generator in the neighbourhood of tuned frequency. Figure 3.6 shows the magnitude frequency response of 1^{st} , 2^{nd} and 3^{rd} order periodic signal generators in the neighbourhood of tuned frequency which is 50 Hz. This figure shows that at 1 percent variation from tuned frequency, the 3^{rd} order generator gives a gain of about 160 dB, whereas the 1^{st} order generator gives a gain of only 50 dB. Also, the gain of 2^{nd} order generator is about 110 dB which is much higher than 50dB³.

²See appendix A.6.

³Note that 50 dB is equal to a gain of 316, where as 110 dB is equal to 316227. Thus, a 1000 times higher gain is offered by the 2^{nd} order generator.

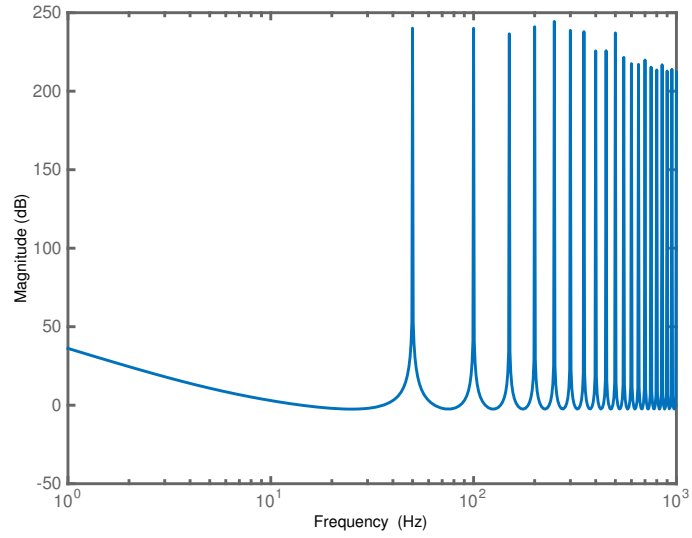


Figure 3.5: Frequency response of 2^{nd} order periodic signal generator.

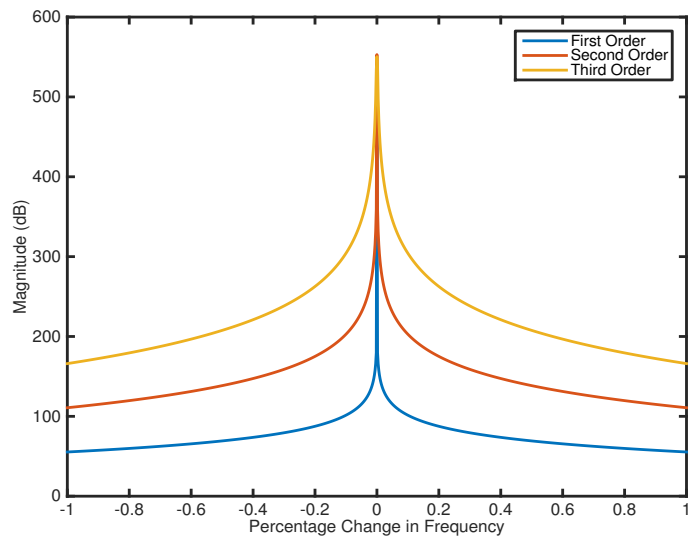


Figure 3.6: Comparison of magnitude frequency response of 1^{st} , 2^{nd} and 3^{rd} order periodic signal generators.

3.3.2 Structure of HORC

The higher order repetitive controller is also used as a plug-in device as shown in figure 3.7. The internal structure of repetitive controller is shown in figure 3.8. In addition to the higher order periodic signal generator, it consists of a lowpass filter $Q(z)$ and a stabilising compensator $G_x(z)$. The lowpass filter attenuates gain at higher harmonics, thus making the stability conditions less stringent. As discussed in chapter 2, the most suitable choice for $Q(z)$ is the first order non-causal finite impulse response filter. It has 0 dB gain at low frequencies and has zero phase. It is given by following equation.

$$Q(z) = 0.25z + 0.5 + 0.25z^{-1} \quad (3.10)$$

$G_x(z)$ is used as a stabilising compensator. It should be designed in such a way that the higher order repetitive controller does not destabilise and degrade the performance of the loop to which it is added.

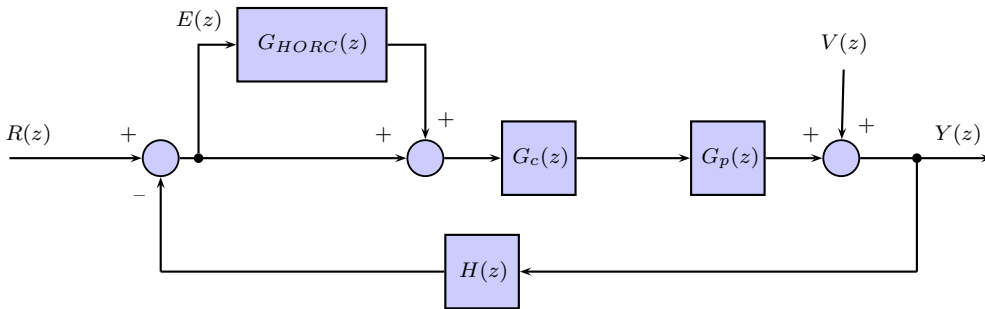


Figure 3.7: Block diagram of generic close-loop control system along with the plug-in repetitive controller.

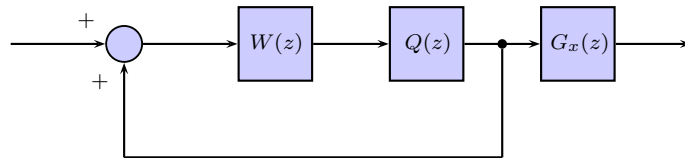


Figure 3.8: Internal structure of higher order plug-in repetitive controller.

3.3.3 Stability Conditions for HORC

Stability conditions for the higher order repetitive control system shown in figure 3.7 can be derived by following the same reasoning as used for the conventional repetitive controller in chapter 2. The sensitivity function for the system shown in figure 3.7 is given by:

$$\frac{Y(z)}{V(z)} = \frac{1}{1 + T(z)} \quad (3.11)$$

Where

$$T(z) = (1 + G_{HORC}(z))G_c(z)G_p(z) \quad (3.12)$$

Here $H(z)$ is taken as unity. From figure 3.8 $G_{HORC}(z)$ is given by:

$$G_{HORC}(z) = \frac{W(z)Q(z)G_x(z)}{1 - W(z)Q(z)} \quad (3.13)$$

Where

$$W(z) = \sum_{l=1}^m w_l z^{-lN} \quad (3.14)$$

The sensitivity function given in (3.11) is simplified⁴ to following form.

$$\frac{Y(z)}{V(z)} = (1 - W(z)Q(z)) \times \frac{1}{1 + G_c(z)G_p(z)} \times \frac{1}{1 + (T_{cl}(z)G_x(z) - 1)W(z)Q(z)} \quad (3.15)$$

The higher order repetitive control system is stable if all the subsystems in the above equation are stable.

1. $1 - W(z)Q(z)$ is stable as $Q(z)$ is a stable lowpass filter. Also, $\|1 - W(z)Q(z)\|_\infty < \infty$.

Thus, this system is H_∞ stable.

2. $\frac{1}{1 + G_c(z)G_p(z)}$ is stable as $G_c(z)$ is designed in such a way that the close loop system without repetitive controller is stable with large margins.

3. $\frac{1}{1 + (T_{cl}(z)G_x(z) - 1)W(z)Q(z)}$ determines the stability of the repetitive control system. The small gain theorem says that this system is stable if $\|(T_{cl}(z)G_x(z) - 1)W(z)Q(z)\|_\infty < 1$. Using the triangular inequality, this condition is modified to $\|(T_{cl}(z)G_x(z) - 1)W(z)Q(z)\|_\infty \leq \|(T_{cl}(z)G_x(z) - 1)W(z)\|_\infty \|Q(z)\|_\infty < 1$.

⁴A detailed step wise simplification is present in appendix A.7.

The above discussion is summarised by the following theorem.

Theorem 4 *The repetitive control system shown in figure 3.7 is stable if*

1. $\|Q(z)\|_\infty \leq 1$
2. $T_{cl}(z)$ is stable.
3. $\|(T_{cl}(z)G_x(z) - 1)W(z)\|_\infty < 1$.

By using $Q(z)$ given by equation (3.10) and $G_x(z) = \frac{K_r}{T_{cl}(z)}$, the repetitive control system can be easily stabilised. However, in many cases where the plant is non-minimum phase or its dynamics are not fully modelled, it becomes impossible to use the inverse of $T_{cl}(z)$ as the stabilising compensator.

3.3.4 Phase Lead Compensation for HORC

In this section it is shown that the phase lead compensator given by following equation can be used to stabilise the higher order repetitive control system shown in figure 3.7.

$$G_x(z) = K_r z^m \quad (3.16)$$

It has already been shown that this compensator adds phase lead to the repetitive control system especially at higher frequencies, thus, compensating the phase lag in the system. In order to develop stability conditions and selection criteria for the parameters of phase lead compensator for the case of higher order repetitive controller, condition 1 and 3 of theorem 4 need to be analysed in detail. Writing condition 1 and 3 together gives.

$$\|(T_{cl}(z)K_r z^m - 1)Q(z)W(z)\|_\infty < 1 \quad (3.17)$$

This condition is reformulated⁵ to following two conditions.

$$|m\Omega + \theta_{T_{cl}}| = 0^\circ \text{ for } 0 < \Omega < \pi \quad (3.18)$$

$$0 < K_r < \frac{\cos(m\Omega + \theta_{T_{cl}})}{M_{T_{cl}}} \text{ for } 0 < \Omega < \pi \quad (3.19)$$

⁵A detailed step by step derivation is given in appendix A.8.

Thus, the stability of higher order repetitive control system using the phase lead compensator is given by following theorem.

Theorem 5 *The repetitive control system shown in figure 3.7 is stable for phase lead compensator given by (3.16) if*

1. $T_{cl}(z)$ is stable.
2. $|m\Omega + \theta_{T_{cl}}| = 0^\circ$ for $0 < \Omega < \pi$
3. $0 < K_r < \frac{\cos(m\Omega + \theta_{T_{cl}})}{M_{T_{cl}}} = K_u$ for $0 < \Omega < \pi$

These conditions can also be used as a design algorithm for phase lead compensator. First, the close loop system is made stable using the conventional PID controller in place of $G_c(z)$. Then condition 2 is satisfied by comparison of the sum of phase angle of the plant and the compensator for various values of m . This comparison gives a suitable value of m . Finally, the range of K_r for which the repetitive control system is stable is determined by plotting K_u against frequency. A suitable K_r is then chosen by analysis of system's bode plot.

It should be noted that condition 2 is very difficult to achieve for a large range of frequency. Therefore, it is expected that the stability margins of the higher order repetitive control system stabilised by phase lead compensator are small.

3.3.5 Higher Order Odd Harmonic Repetitive Controller

Similar to conventional repetitive controller, the only difference between higher order and odd harmonic higher order repetitive controller is that of the periodic signal generator[19]. The signal generator used by the odd harmonic higher order repetitive controller is given by following equation.

$$W(z) = \sum_{l=1}^m (-1)^{l-1} w_l z^{-l\frac{N}{2}} \quad (3.20)$$

The weights of this generator are also evaluated by the same procedure as described in section 3.3.1. The magnitude frequency response of a 2^{nd} order odd harmonic periodic signal generator is shown in figure 3.9. It is evident that this generator gives high gain only at odd harmonics of the tuned frequency which is 50 Hz in this case.

The stability conditions given in theorem 4 and 5 are also applicable to higher order odd harmonic repetitive controller.

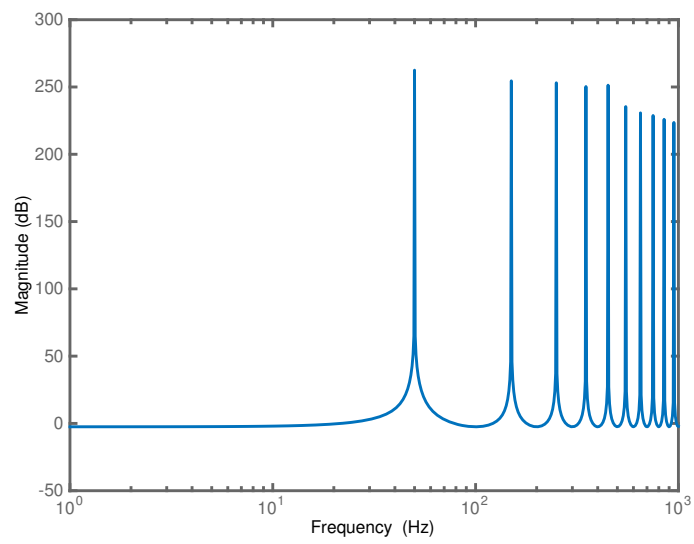


Figure 3.9: Frequency response of 2^{nd} order odd harmonic periodic signal generator tuned at 50 Hz.

Chapter 4

Robust High Order Repetitive Control of Two Level Grid Connected Converter

4.1 Introduction

This chapter discusses the implementation of repetitive and higher order repetitive controller for harmonic rejection in two level grid connected converter. The reason for choosing a grid connected converter for the validation of ideas presented in this thesis is that the grid connected converters are the backbone of microgrids. A microgrid is a localised grouping of electricity sources which is connected to the centralised grid (macrogrid), but it can also disconnect and function autonomously as physical and/or economic conditions dictate¹. Thus, a microgrid enables a small scale independent power producer to generate electricity for its own needs and sell the surplus power to the national power company.

Pakistan is facing an acute energy crisis. This crisis has two facets. One is the large difference between the production capacity and consumption. The other facet is the decades old transmission and distribution system. Even if the shortfall gap is narrowed by adding new power plants, the transmission and distribution system cannot bear the load without break. For this situation, the small scale distributed production from renewable energy sources is a very suitable answer. Consumers can generate locally and feed the surplus to national grid. Of

¹<https://building-microgrid.lbl.gov/about-microgrids>

course, the details and viability of this solution need to be investigated in great detail. However, keeping in view the promise that the microgrid has shown in other countries[20], the idea of microgrid is worth giving time and effort.

A number of converter topologies exist which can be used as grid connected converters[21]. Table 4.1 compares a number of converters which are commonly used. The two level voltage source converter with LCL filter is chosen for this work because of its simplicity and wide application. The particular design of two level converter being used was developed by Abusara et al.[22].

The motivation for using repetitive controller for grid connected converter comes from the fact that the conventional PID controller fails when the grid voltage has high harmonic content. A detailed investigation of this phenomenon and implementation of repetitive controller for two level converter can be found in [23].

In the following sections, the repetitive controller is reimplemented for the two level converter using the same approach as used in [23]. Then, it is shown that the designed controller works perfectly well under high harmonics as long as the frequency of the grid does not change. Next, it is shown that the designed controller fails under variation in grid frequency. Finally, a robust high order repetitive controller is designed and implemented using the techniques discussed in chapter 3. Simulations are carried out for linear model of two level converter to prove that the proposed controller gives desired performance under frequency variation.

Table 4.1: Comparison of converter used in this work with other converters.

No.	Converter	Merit	Demerit
1	Two level voltage source converter with LCL filter (used in this work)	Small filter size Good output THD	Requires complex control technique to avoid resonance
2	Two level voltage source converter with L filter	First order system Easy to control	Large filter size Poor output THD
3	Two level voltage source converter with LCCL filter	No filter resonance Easy to control Good output THD	Larger filter size
4	Multi level voltage source converter with LCL filter	Smaller filter size Good output THD	Very expensive power electronics and Complex control
5	Interleaved converter	Smallest filter size Good output THD Small but fast electronic components	Complex control Large number of electronic components

4.2 Evaluation Criteria

The controllers designed and implemented in subsequent sections are evaluated by simulations on MATLAB/SIMULINK. The evaluation criteria for the implemented controllers is:

1. The reference current is 100 amperes. The frequency and phase of the reference current is synchronised with the grid. It means that if the grid frequency changes, the reference frequency also changes with it.
2. The maximum total harmonic distortion (THD) allowed[24] in output current is given in table 4.2. If the output current has higher harmonic content than this for any controller, that controller is considered failure.
3. Table 4.3 specifies two cases for grid voltage. The first case is from a real grid[23]. It represents normal harmonic content. The second case is artificial. It represents a grid with high harmonic content. A controller is first tested for case I; if it is successful, then it is tested for case II.

Table 4.2: Harmonic currents limits according to ANSI/IEEE standard 519-1992.

Odd Harmonic Order 'n'	$n \leq 11$	$11 < n \leq 17$	$17 < n \leq 23$	$23 < n \leq 35$	$n > 35$	THD
Percentage of fundamental	4	2	1.5	0.6	0.3	5.0 %

Table 4.3: Two cases for grid voltage harmonics. The first case was measured at a test site in Exeter University, U.K.

	Case I	Case II
Harmonic Number 'n'	Amplitude V(rms)	Amplitude V(rms)
Fundamental	230	230
3^{rd}	2.4	18.4
5^{th}	4.22	11.5
7^{th}	1.95	9.2
9^{th}	2.37	4.6
11^{th}	1.46	0.115
13^{th}	1.95	0.057
15^{th}	0.455	0.23
17^{th}	0.65	0.23
19^{th}	0.585	0.23
THD	2.74%	10.44%

4.3 Two Level Converter

A detailed description of the two level converter used here can be found in [22][23]. Figure 4.1 shows the block diagram of two level converter connected in close-loop. Here $I_2(s)$ is the output current of a single phase of the converter. $V_u(s)$ is the grid voltage. This is the point where harmonics enter the system as disturbance. Following equations give the plant and disturbance transfer functions.

$$G_p(s) = \frac{1}{(L_1L_2C)s^3 + K_cL_2Cs^2 + (L_1 + L_2)s} \quad (4.1)$$

$$D(s) = L_1Cs^2 + K_cCs + 1 \quad (4.2)$$

The parameters and component values for the two level converter are given in table 4.4.

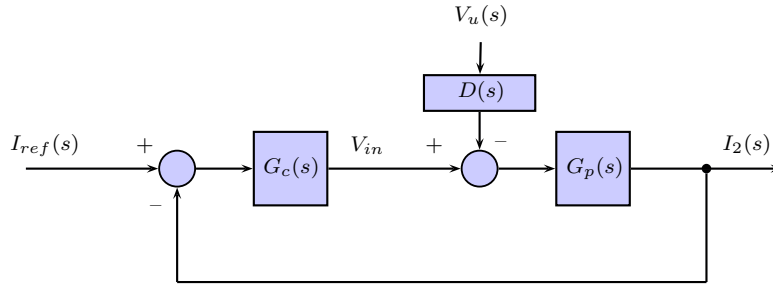


Figure 4.1: Block diagram of two level converter with conventional controller.

Before applying repetitive controller, it is required that the close-loop system be made stable using a conventional PID controller.

Table 4.4: System parameters and component values for the two level grid connected converter with LCL filter.

Parameter	Description	Value
V_u	Utility phase voltage	230 V(rms)
V_{DC}	DC link voltage	750 V DC
L_1	1 st inductor of filter	350 μ H
L_2	2 nd inductor of filter	50 μ H
C	Filter capacitance	160 μ F
K_c	Inner loop gain	13
F_s	Switching frequency	8 KHz
F_g	Grid frequency	50 Hz
f_s	Sampling frequency	20 KHz
N	No. of samples per period	400
P_{inv}	Rated power	80 KVA

4.3.1 Conventional PID Controller

In order to design a PID controller for the two level converter, its frequency response is analysed². Figure 4.2 shows the frequency response of transfer function from $I_2(s)$ to $V_{in}(s)$. It is evident from this plot that the system has large stability margins. Also, the system has large D.C. gain. However it has small bandwidth. Its bandwidth is just 398 Hz. In order to improve the bandwidth, a simple proportional controller is used. Its gain is selected by inspection. The convention controller for two level converter is given by following equation.

$$G_c(s) = 4 \quad (4.3)$$

Figure 4.3 shows the frequency response of the converter along with the designed proportional controller. Now, the system has large stability margins and its bandwidth has also improved to 1.62 KHz.

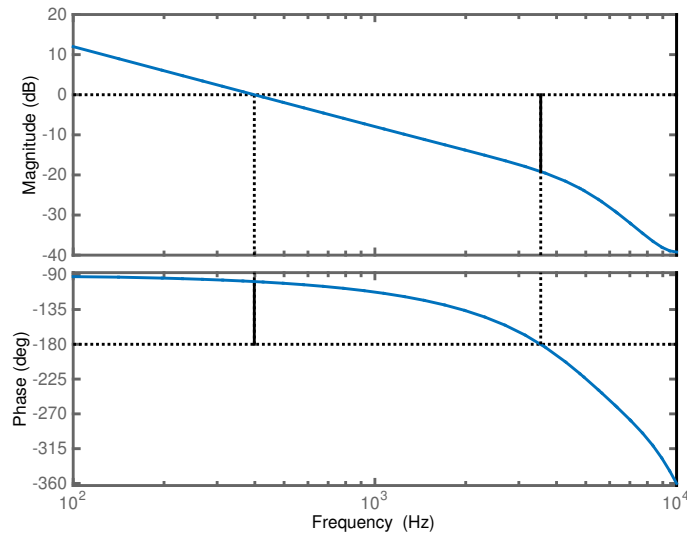


Figure 4.2: Frequency response of converter transfer function. The gain margin is 19.1 dB, the phase margin is 81.2 degrees and system bandwidth is 398 Hz.

4.3.2 Testing the PID Controller

The designed PID controller is test on the linear model shown in figure 4.1. Figure 4.4 shows the output current of the converter controlled by PID. The grid voltage is as of case I. The THD of the output current is 2.74%. Clearly the output THD is less than 5%, which means

²All the plots shown here are obtained by using the discrete time representation of the system. This is done to preempt any problems during the design of repetitive controller which is implemented in discrete domain.

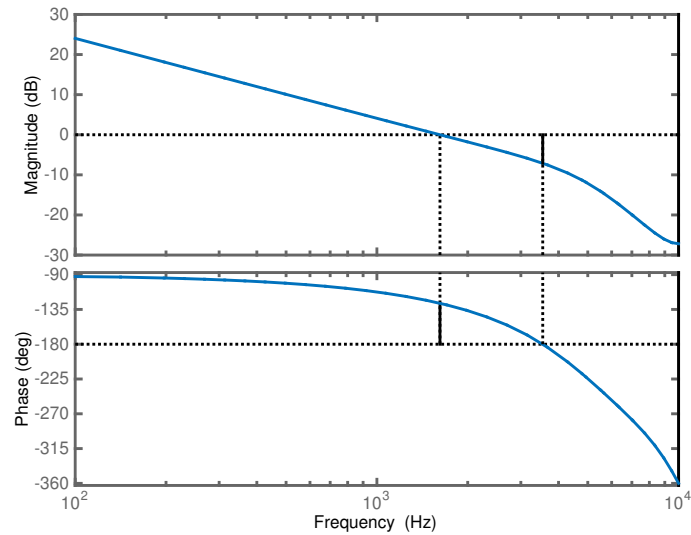


Figure 4.3: Frequency response of converter transfer function along with proportional controller. The gain margin is 7.11, the phase margin is 52.9 degrees and system bandwidth is 1.62 KHz.

that the PID controller has passed the test for case I. However, it should be noted that the voltage THD for case I is also small, i.e. 2.74%.

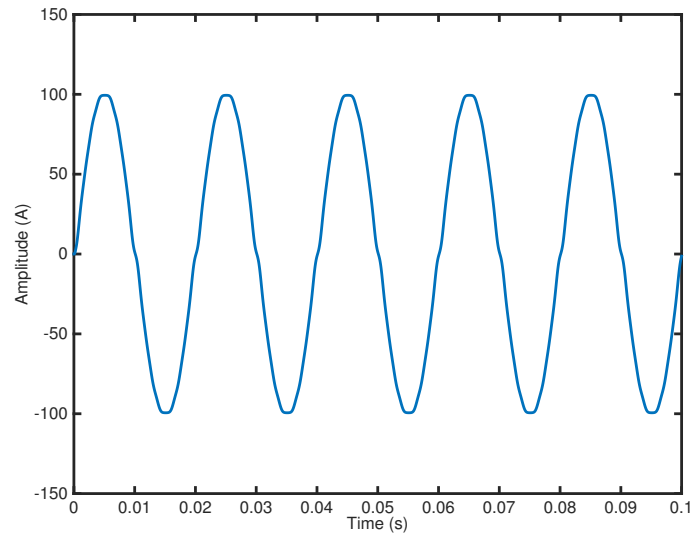


Figure 4.4: Output current of the converter controlled by PID. The grid voltage is as of case I and the current THD is 2.74%.

Figure 4.5 shows the output current for case II of grid voltage. Here, the output current THD is 10.38%. It is well above 5%. Observing the output current THD for the both cases it seems that the PID controller is doing nothing for rejection of the disturbances which are higher harmonics in this case. Both the grid voltage and output current have almost same harmonic content. Thus, the PID controller fails under high harmonics in the grid.

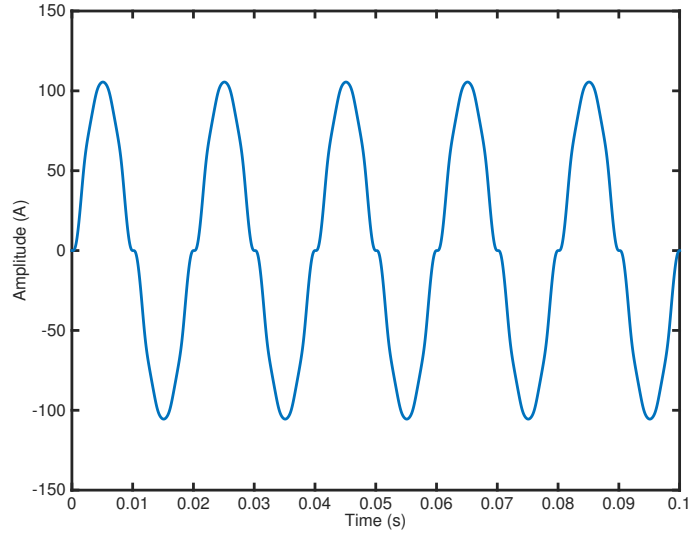


Figure 4.5: Output current of the converter controlled by PID. The grid voltage is as of case II and the current THD is 10.38%.

4.4 Conventional Repetitive Controller

In this section a conventional odd harmonic repetitive controller is designed for the two level converter. Odd harmonic repetitive controller is chosen because of the fact that the grid only contains odd harmonics. Figure 4.6 shows the two level converter and an odd harmonic repetitive controller connected in close loop. The internal structure of the odd harmonic repetitive

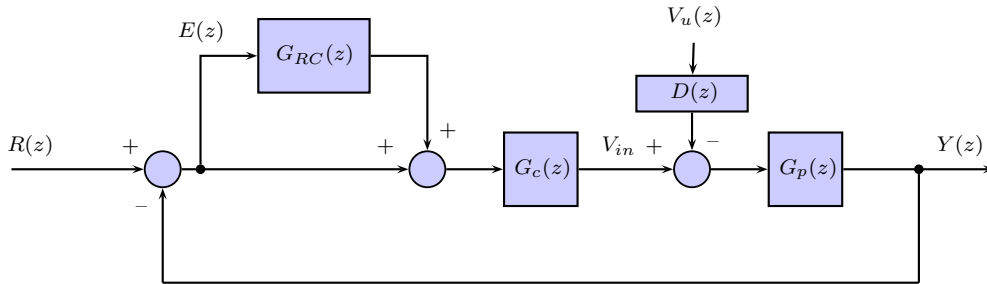


Figure 4.6: Block diagram of two level converter with repetitive controller.

controller is shown in figure 4.7. Note that a phase lead compensator is being used instead of inverse compensator. It is because of the fact that the plant is non-minimum phase and, thus, its inverse is an unstable system. Figure 4.8 shows the pole zero map of the converter transfer function.

The odd harmonic repetitive controller can be designed for the two level converter by satisfying the conditions of theorem 3 from chapter 2. Its conditions are given below.

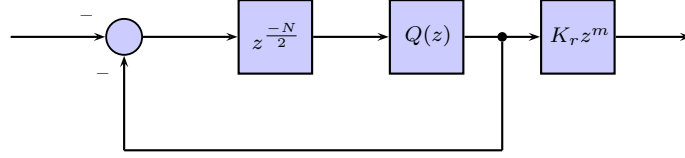


Figure 4.7: Internal structure of odd harmonic repetitive controller used for the two level converter.

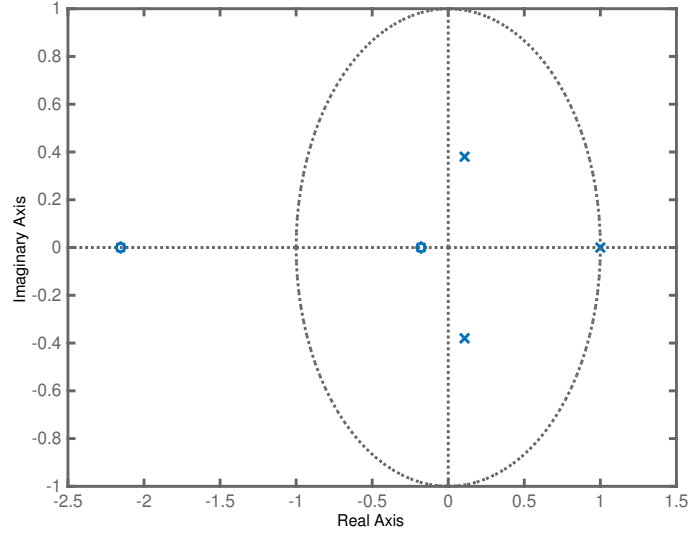


Figure 4.8: Pole zero map for the converter transfer function. The zero outside the unit circle indicates that the system is non-minimum.

1. $\|Q(z)\|_{\infty} \leq 1$
2. $T_{cl}(z)$ is stable.
3. $0 < K_r < \frac{2\cos(\theta_{T_{cl}}(e^{j\Omega}) + m\Omega)}{M_{T_{cl}}(e^{j\Omega})} = K_u$ for all Ω
4. $|\theta_{T_{cl}}(e^{j\Omega}) + m\Omega| < 90^\circ$ for all Ω

Condition 1 can be satisfied by using following non-causal moving average filter.

$$Q(z) = 0.25z + 0.5 + 0.25z^{-1} \quad (4.4)$$

Condition 2 is satisfied as the close loop system without the repetitive controller is stable. $T_{cl}(z)$ is given by:

$$T_{cl}(z) = \frac{G_c(z)G_p(z)}{1 + G_c(z)G_p(z)} \quad (4.5)$$

The pole zero map of $T_{cl}(z)$ is shown in figure 4.9. This map shows that all the poles are within the unit circle. Thus, $T_{cl}(z)$ is stable. Also, it has already been shown in figure 4.3 that

$G_c(z)G_p(z)$ has large stability margins, therefore, the corresponding close loop system $T_{cl}(z)$ is stable. In order to satisfy condition 3 and 4, suitable values of K_r and m need to be selected.

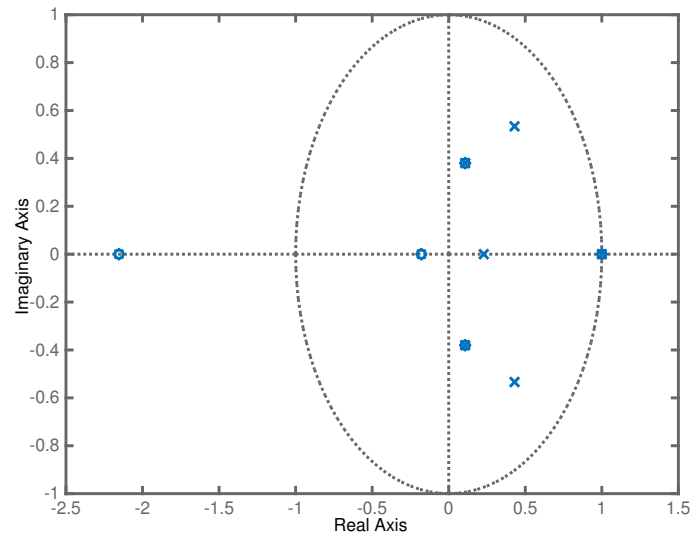


Figure 4.9: Pole zero map for $T_{cl}(z)$

First, an appropriate value of m is selected by analysing the joint phase plot of T_{cl} and z^m for various values of m . Figure 4.10 shows such a plot. From this plot; it is clear that for $m = 2$, condition 4 is satisfied upto Nyquist frequency 10 KHz. Thus, 2 is the most suitable choice for m . Now, only condition 3 need to be satisfied. To determine the range of K_r for which the system is stable, the plot of K_u against frequency is considered. Figure 4.11 shows plot of K_u against frequency. The minimum value of K_u is 1.2. Thus, K_r can be selected in the range (0,1.2). The exact value of K_r is chosen by inspection of the bode plot of the system. In order to have large stability margin, K_r is selected as 0.1. Also, $G_c(z)$ is readjusted to 3 for an increase in the phase margin of the system.

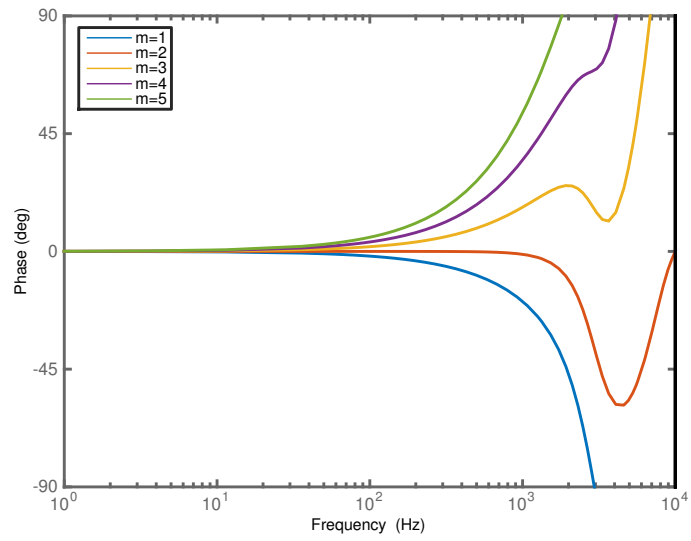


Figure 4.10: Frequency phase plot of $T_{cl}(z)z^m$ for various values of m .

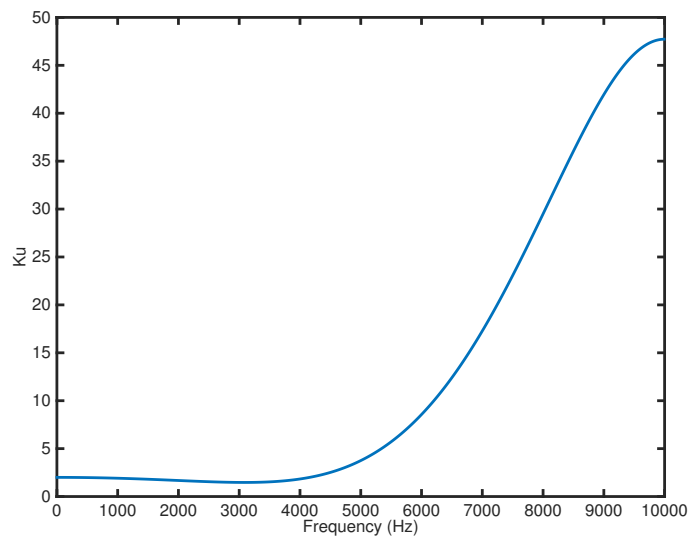


Figure 4.11: Frequency magnitude plot of K_u . The minimum value of K_u is 1.2.

4.4.1 Analysis of Designed Controller

Following is a list of the selected repetitive controller parameters.

1. $N = 400$
2. $Q(z) = 0.25z + 0.5 + 0.25z^{-1}$
3. $K_r = 0.1$
4. $m = 2$
5. $G_c(z) = 3$

Figure 4.12 shows the frequency response of converter transfer function along with the designed odd harmonic repetitive controller. The system has robust stability margins. It also offers large gains at the fundamental frequency and its harmonics. In order to better appreciate the

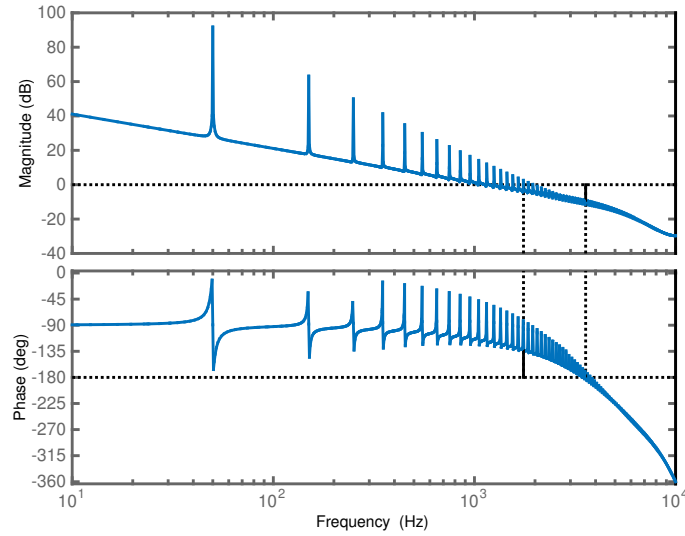


Figure 4.12: Frequency response of two level converter along with the designed conventional odd harmonic repetitive controller. The gain margin is 9.14 dB. The phase margin is 46 degrees.

disturbance rejection capability of the system, the disturbance transfer function of the system is analysed. The disturbance transfer function is given by:

$$G_D(z) = \frac{I_{ref}(z)}{V_u(z)} = \frac{G_p(z)D(z)}{1 + G_p(z)G_c(z)(1 + G_{RC}(z))} \quad (4.6)$$

The bode plot of disturbance transfer function is given in figure 4.13. This plot shows that the system bandwidth is about 1 KHz. It means that the system can reject disturbances upto 1

KHz. It is also clear that the system offers high attenuation to disturbances of 50 Hz and its harmonics upto 1 KHz, i.e. 19th harmonic.

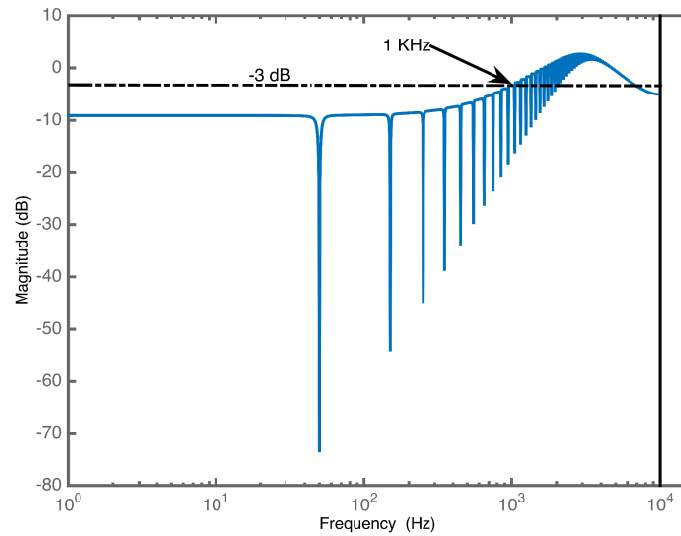


Figure 4.13: Frequency response of the disturbance transfer function. System bandwidth is about 1 KHz.

4.4.2 Testing the Conventional Repetitive Controller

The conventional repetitive controller is tested for the two cases of grid voltage on the linear model by SIMULINK simulations. The repetitive controller successfully rejects harmonics and the output current THD for both case is 0.23%. Figure 4.14 shows the output current of the converter for case II grid voltage.

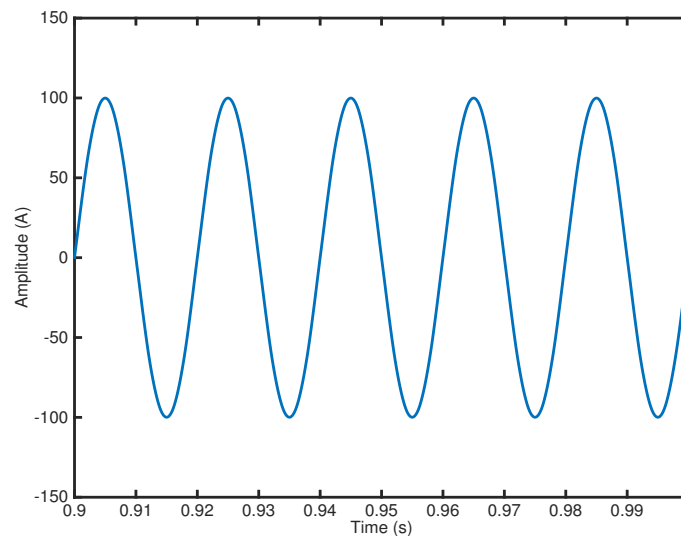


Figure 4.14: Converter output current for case II grid voltage. The THD is just 0.23%. Thus, repetitive controller successfully rejects odd harmonics in the grid.

4.4.3 Performance under Frequency Variation

In order to test the performance of conventional repetitive controller under frequency variation, the frequency of the grid is varied by 1%. This amount of variation in grid frequency is allowed by international standards. Therefore, this much variation is expected in the grid. The controller is tested at 49.5 Hz grid frequency for both cases of grid voltage. For case I the output current THD is 3.12%, which is within the allowed range. However, for case II the current THD is 10.56%. It is worse than the PID controller. In fact, the variation in frequency has rendered the repetitive controller ineffective. It was discussed in chapter 2 that the conventional repetitive controller offers little attenuation in the neighbourhood of tuned frequency and its harmonics. Figure 4.15 shows the output current of the converter for case II grid voltage when grid frequency is 49.5 Hz.

This discussion shows that the repetitive controller fails to perform under frequency variation. In the following section a robust high order odd repetitive controller is designed which caters to variations in grid frequency and its performance does not degrade under frequency variation.

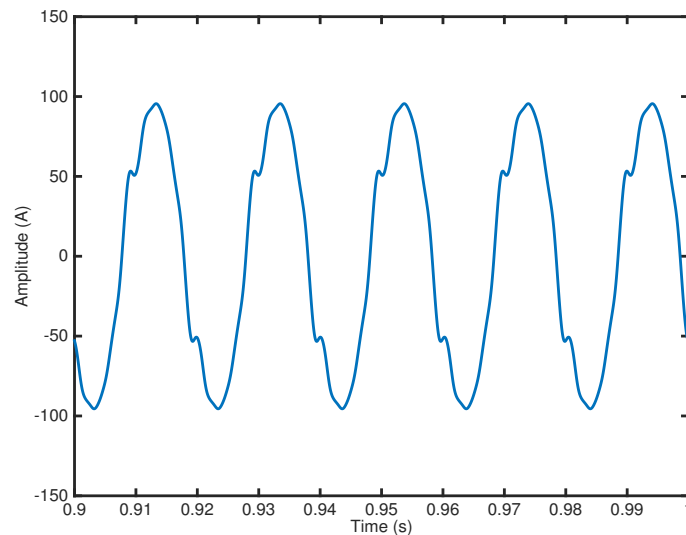


Figure 4.15: Converter output current for case II grid voltage in the presence of 1% variation in grid frequency. The THD is 10.56%. Thus, repetitive controller fails to reject odd harmonics in the grid under frequency variation.

4.5 2^{nd} Order Odd Harmonic Repetitive Controller

In this section, a robust 2^{nd} order odd harmonic repetitive controller is designed for the two level converter. As it has been shown that the converter is a non-minimum phase system, thus, inverse model compensator cannot be used. The 2^{nd} order repetitive controller is given by following equation.

$$G_{horc} = \frac{-W(z)Q(z)G_x(z)}{1 + W(z)Q(z)} \quad (4.7)$$

Where

$$W(z) = 2z^{-N/2} + z^{-N} \quad (4.8)$$

$Q(z)$ is chosen as the low pass first order non-causal filter.

$$Q(z) = 0.25z + 0.5 + 0.25z^{-1} \quad (4.9)$$

N is evaluated by the following expression.

$$N = \frac{20000}{50} = 400 \quad (4.10)$$

The phase lead compensator $K_r z^m$ is designed by satisfying the conditions of theorem 5 from chapter 3. The conditions are given below.

1. $T_{cl}(z)$ is stable.
2. $|m\Omega + \theta_{T_{cl}}| = 0^\circ$ for $0 < \Omega < \pi$
3. $0 < K_r < \frac{\cos(m\Omega + \theta_{T_{cl}})}{M_{T_{cl}}} = K_u$ for $0 < \Omega < \pi$

Condition 1 is satisfied by making the close loop system without the repetitive controller stable with $G_c(z) = 3$. It has already been shown that $T_{cl}(z)$ has large stability margins for $G_c(z) = 3$.

In order to satisfy condition 2, an appropriate value of m has to be selected. This selection is made by comparing the phase of $T_{cl}(z)z^m$ for various values of m . Figure 4.16 shows a plot of the phase of $T_{cl}(z)z^m$ for different values of m . From this figure, it is evident that the phase remains closer to zero for $m = 2$. Thus, 2 is the most suitable value for m . However, it should

be noted that this value of m does not satisfy condition 2 for all ω such that $0 < \Omega < \pi$. Therefore, it is expected that the stability margins of the repetitive control system are very small. Finally, K_r is selected from condition 3. Figure 4.17 shows a plot of K_u against

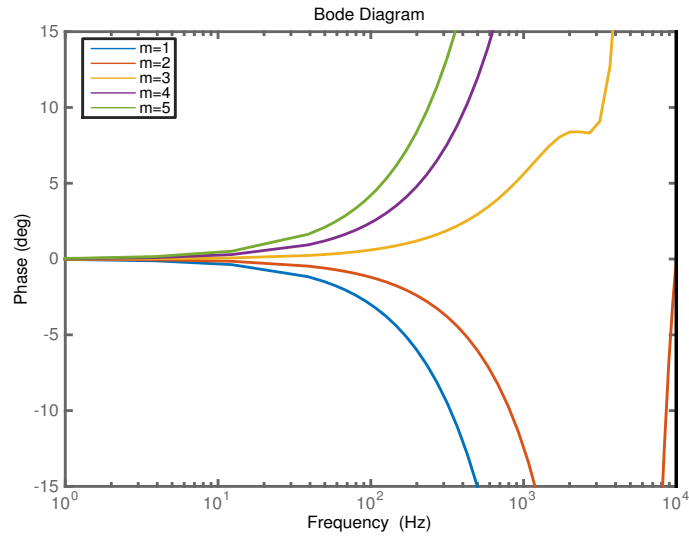


Figure 4.16: Frequency phase plot of $T_d(z)z^m$ for various values of m .

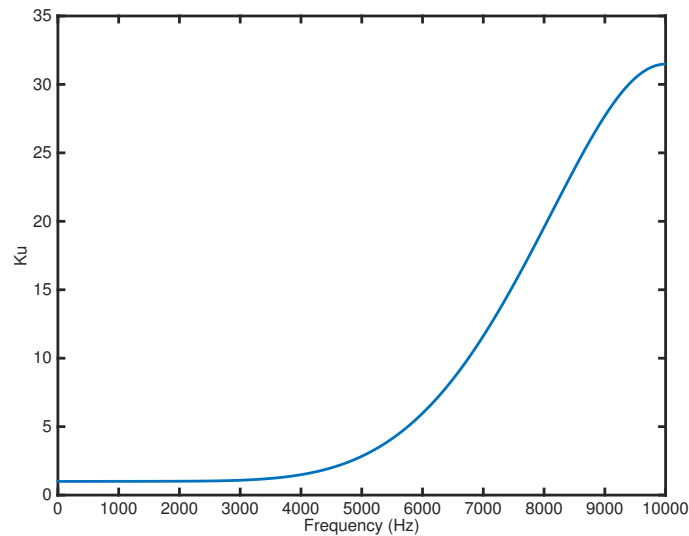


Figure 4.17: Frequency magnitude plot of K_u . The minimum value of K_u is 1.

frequency. The minimum value of K_u is 1. Thus, K_r can be selected in the range $(0, 1)$. The exact value of K_r is chosen so that the repetitive control system has maximum stability margins. A smaller value of K_r gives higher stability margins. However, the value of K_r also affects the gain of repetitive controller at and around the tuned frequency and its harmonics. Figure 4.18 shows a comparison of different value of K_r . From this figure it is clear that a smaller value of K_r means that the gain of repetitive controller at and around the tuned frequency is smaller. And a smaller gain results in poor disturbance rejection and tracking.

Therefore, a compromise value of K_r has to be selected which gives adequate stability margin along with desired gain at and around the tuned frequency. By this reasoning, K_r is selected as 0.3. Figure 4.19 shows the frequency response of the converter along with the designed 2nd

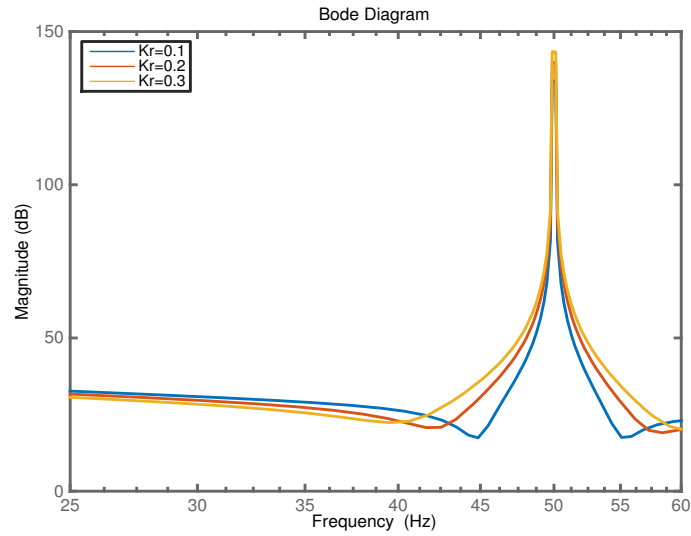


Figure 4.18: Frequency magnitude plot of converter along with the 2nd order repetitive controller for different values of K_r .

order repetitive controller. Although the system is stable but has very small gain and phase margins as predicted by condition 2 of theorem 5. It can become unstable with small changes in grid impedance. Figure 4.20 shows the frequency response of converter's disturbance transfer function for the 2nd order repetitive controller. The bandwidth of the system is only 60 Hz. However, it should be noted that the low bandwidth does not degrade the periodic performance of the system as the system has high attenuation at the tuned frequency and its harmonics. It only degrades the non periodic performance. The degradation in non-periodic performance means that the settling time and rise time of the system are poor and the system might have steady state error.

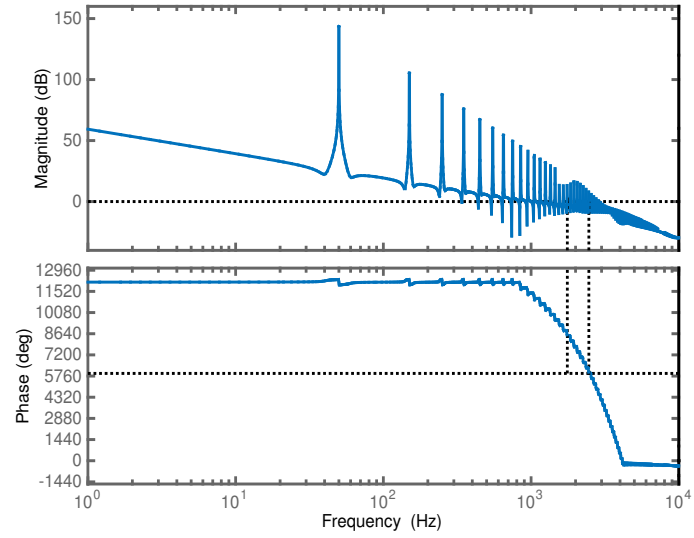


Figure 4.19: Frequency response of two level converter alongwith the designed 2^{nd} odd harmonic repetitive controller. The gain margin is -2.13 dB. The phase margin is 6.01 degrees.

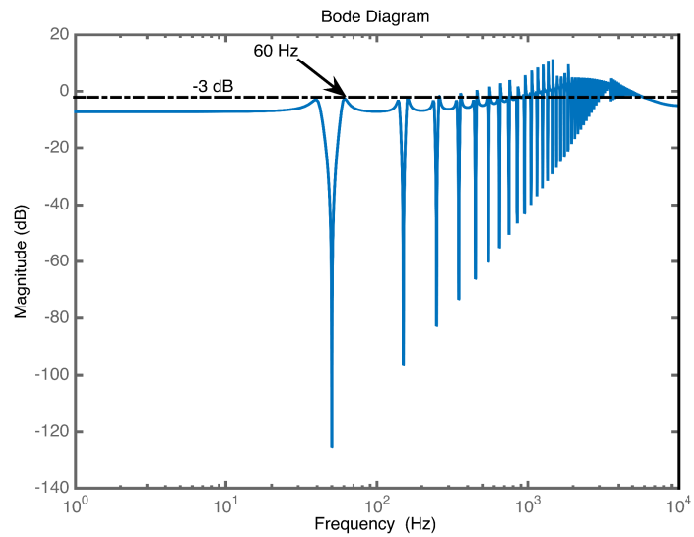


Figure 4.20: Frequency response of the disturbance transfer function. System bandwidth is about 60 Hz.

4.5.1 Modified Compensator

The designed compensator $G_x(z)$ is modified in order to improve the stability margins of the system. The modified compensator is given below.

$$G_x(z) = 0.3(z^2 + z^4) \tag{4.11}$$

Figure 4.21 shows the frequency response of the converter transfer function along with the 2nd order odd harmonic repetitive controller with the modified compensator. Both the phase margin and gain margin have improved considerably. Figure 4.22 shows that the bandwidth of the system is now at 230 Hz.

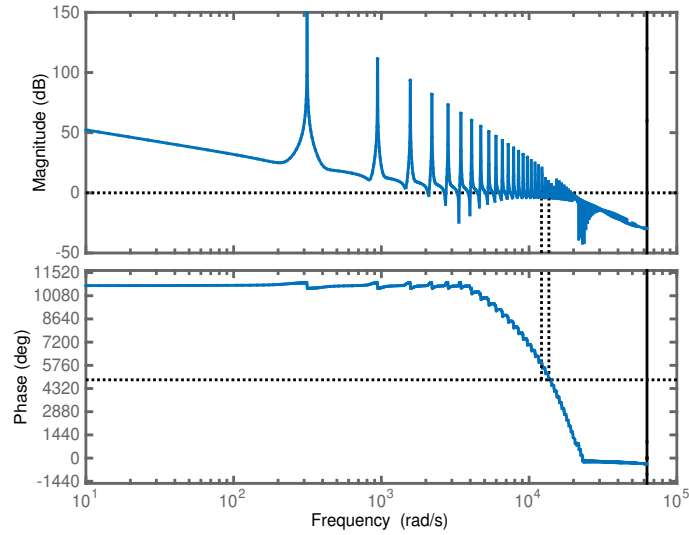


Figure 4.21: Frequency response of two level converter along with the designed 2nd order odd harmonic repetitive controller with the modified compensator. The gain margin is 3.67 dB. The phase margin is 27.1 degrees.

4.6 Testing the Performance

The performance of the 2nd order repetitive controller is tested for case II of grid voltage at 50 Hz and 49.5 Hz by simulating the linear model. At 50 Hz, the output current THD is 0.04%. At 49.5 Hz the current THD is 2.18%. Figure 4.23 shows the output current for case II grid voltage when grid frequency is 49.5 Hz. Therefore, the higher order odd harmonic repetitive controller successfully rejects harmonics even under the presence of frequency variation in the grid.

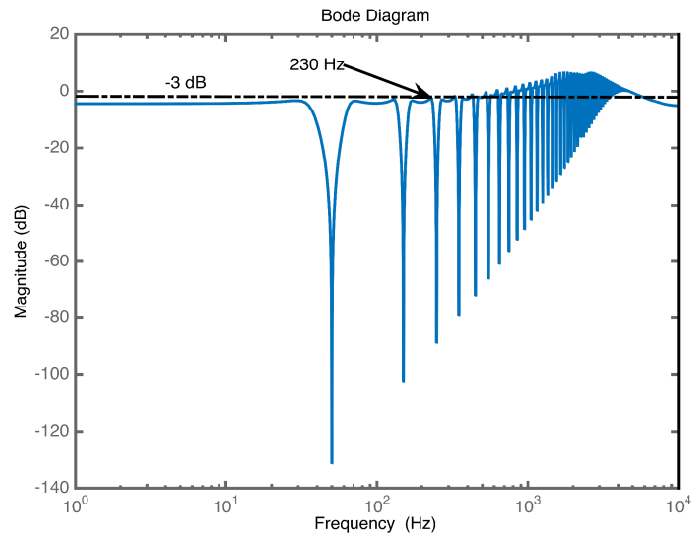


Figure 4.22: Frequency response of the disturbance transfer function. System bandwidth is about 230 Hz.

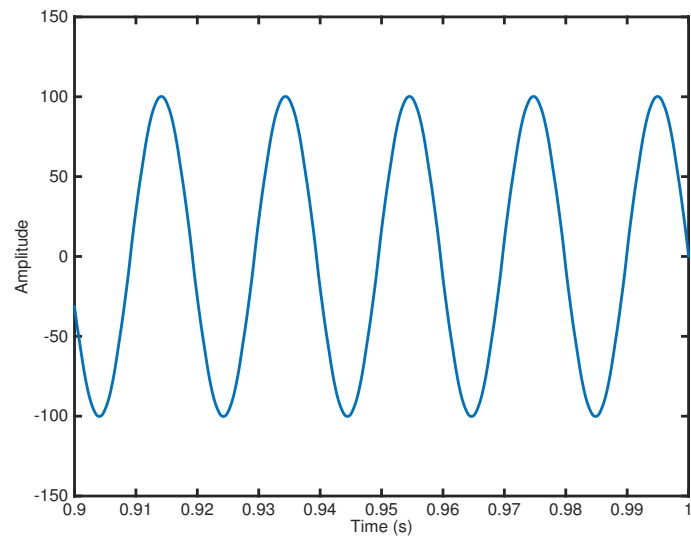


Figure 4.23: Converter output current for case II grid voltage in the presence of 1% variation in grid frequency. The controller is 2^{nd} order odd harmonic repetitive controller with the compensator given by (4.11). The current THD is 2.18%.

4.7 Comparison of Results

Table 4.5 shows the output current THD of the two level converter for different controllers under various conditions of grid voltage. It is clear that the 2^{nd} order repetitive controller shows best result under all conditions.

Table 4.5: Comparison of output current THD for different controllers.

No.	Controller	Current THD for grid voltage case II at 50 Hz	Current THD for grid voltage case II at 49.5 Hz
1	PID controller	10.38%	10.38%
2	Repetitive controller	0.23%	10.56%
3	2^{nd} order repetitive controller	0.04%	2.18%

Chapter 5

Conclusion and Future Work

5.1 Conclusion

The core objective of this thesis was to analyse the performance degradation of the repetitive controller under frequency variation and find out a solution to this problem. This thesis started from the very basics of control theory. The repetitive controller was introduced and all its components were explained and motivated. The stability conditions for the repetitive controller were derived and the derivation was presented in detail. It was shown, theoretically, that the repetitive controller fails under frequency variation. In chapter 4, this phenomenon was also discussed for two level grid connected converter.

Chapter 3 explored two solutions for improving the performance of repetitive controller under frequency variation. The first solution was the adaptive repetitive controller. The second solution was higher order repetitive controller. The stability and design of higher order repetitive controller was discussed in detail. The stability conditions were derived. A major development in this chapter was that of the extension of phase lead compensation to higher order repetitive controller. The phase lead compensation allowed the implementation of higher order repetitive controller for non-minimum phase systems. The derived stability conditions were used to design a higher order repetitive controller using phase lead compensation for two level converter in chapter 4.

The problem, however, is that the stability conditions for phase lead compensator used for higher order repetitive controller are very strict. These stringent stability conditions result in small stability margins. In chapter 4, it was observed that the prediction of small stability

margins is indeed true. This problem was solved for the case of two level converter system by slightly modifying the designed compensator. However, a general solution has to be found.

5.2 Future Work

In view of the work done in this thesis, following are the potential avenues for further research.

1. Implementation of the proposed higher order repetitive controller with phase lead compensator on a real two level grid connected converter.
2. Analysis of the modified phase lead compensator $K_r(z^m + z^{2m})$ which showed substantial improvement in stability margins for the case of two level grid connected converter.
3. Recently Kurniawan et al. [15] have proposed an IIR stabilising compensator for conventional repetitive controller. This compensator might show promising results when applied to stabilise a higher order repetitive control system.

Appendix A

Derivation of Formulae

A.1 Close Loop System's Error

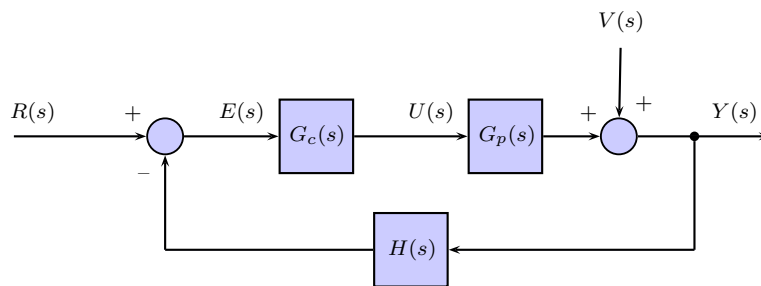


Figure A.1: Block diagram of generic close loop control system.

The error $E(s)$ of the system shown in figure A.1 is given by:

$$E(s) = R(s) - H(s)Y(s) \quad (\text{A.1})$$

Where

$$Y(s) = V(s) + G_p(s)G_c(s)E(s) \quad (\text{A.2})$$

Substituting $Y(s)$ into equation (A.1) gives:

$$E(s) = R(s) - H(s)V(s) - H(s)G_p(s)G_c(s)E(s) \quad (\text{A.3})$$

Where

$$T(s) = G_c(s)G_p(s)H(s) \quad (\text{A.4})$$

Substituting $T(s)$ in equation (A.3) gives:

$$E(s) = R(s) - H(s)V(s) - T(s)E(s) \quad (\text{A.5})$$

Further simplification gives:

$$E(s) = \frac{R(s)}{1 + T(s)} - \frac{H(s) \times V(s)}{1 + T(s)} \quad (\text{A.6})$$

A.2 Discrete Periodic Signal Generator

The transfer function of continuous-time periodic signal generator is given by:

$$G_{im}(s) = \frac{e^{-T_p s}}{1 - e^{-T_p s}} \quad (\text{A.7})$$

The following relation maps the s-plane onto z-plane.

$$z = e^{sT_s} \quad (\text{A.8})$$

The number of samples per period in discrete domain is given by:

$$N = \frac{T_p}{T_s} \quad (\text{A.9})$$

Rewriting above equation gives:

$$T_p = NT_s$$

Substituting T_p in equation (A.7) gives:

$$G_{im}(s) = \frac{e^{-sNT_s}}{1 - e^{-sNT_s}} \quad (\text{A.10})$$

Rewriting above equation gives:

$$G_{im}(s) = \frac{(e^{sT_s})^{-N}}{1 - (e^{sT_s})^{-N}} \quad (\text{A.11})$$

Substituting e^{sT_s} from equation (A.8) in equation (A.11) gives:

$$G_{im}(z) = \frac{z^{-N}}{1 - z^{-N}} \quad (\text{A.12})$$

A.3 Fourier Series Formulation

The Fourier series¹ for a periodic signal $f(t)$ over interval $[0, T_p]$ is given by:

$$f(t) = \frac{a_o}{2} + \sum_{n=1}^{\infty} a_n \cos\left(\frac{2\pi nt}{T_p}\right) + b_n \sin\left(\frac{2\pi nt}{T_p}\right) \quad (\text{A.13})$$

The Fourier coefficients are given by:

$$a_o = \frac{2}{T_p} \int_0^{T_p} f(t) dt \quad (\text{A.14})$$

$$a_n = \frac{2}{T_p} \int_0^{T_p} f(t) \cos\left(\frac{2\pi nt}{T_p}\right) dt \quad (\text{A.15})$$

$$b_n = \frac{2}{T_p} \int_0^{T_p} f(t) \sin\left(\frac{2\pi nt}{T_p}\right) dt \quad (\text{A.16})$$

Considering following new variables:

$$A_o = a_o$$

$$a_n = A_n \sin(\phi_n)$$

$$b_n = A_n \cos(\phi_n)$$

Substituting these variables in equation (A.13) gives:

$$f(t) = \frac{A_o}{2} + \sum_{n=1}^{\infty} A_n \sin(\phi_n) \cos\left(\frac{2\pi nt}{T_p}\right) + A_n \cos(\phi_n) \sin\left(\frac{2\pi nt}{T_p}\right) \quad (\text{A.17})$$

¹Weisstein, Eric W. "Fourier Series." From MathWorld—A Wolfram Web Resource. Available at: <http://mathworld.wolfram.com/FourierSeries.html>

Using the following trigonometric identity:

$$\sin(\alpha + \beta) = \sin(\alpha)\cos(\beta) + \cos(\alpha)\sin(\beta) \quad (\text{A.18})$$

Equation (A.17) becomes:

$$f(t) = \frac{A_o}{2} + \sum_{n=1}^{\infty} A_n \sin\left(\frac{2\pi nt}{T_p} + \phi_n\right) \quad (\text{A.19})$$

Where

$$a_n^2 + b_n^2 = (A_n \sin(\phi_n))^2 + (A_n \cos(\phi_n))^2 = A_n^2 (\sin^2(\phi_n) + \cos^2(\phi_n)) = A_n^2$$

Therefore

$$A_n = \sqrt{a_n^2 + b_n^2} \quad (\text{A.20})$$

And

$$\frac{a_n}{b_n} = \frac{A_n \sin(\phi_n)}{A_n \cos(\phi_n)} = \tan(\phi_n)$$

Therefore

$$\phi_n = \tan^{-1}\left(\frac{a_n}{b_n}\right) \quad (\text{A.21})$$

A.4 Sensitivity Function of Repetitive Control System

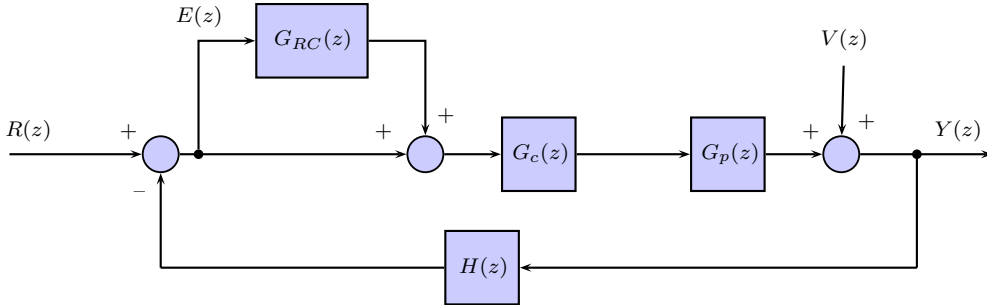


Figure A.2: Block diagram of generic close loop control system along with the plug-in repetitive controller.

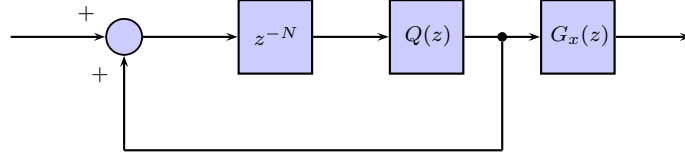


Figure A.3: Internal structure of plug-in repetitive controller.

The sensitivity function for the system shown in figure A.2 is given by:

$$\frac{Y(z)}{V(z)} = \frac{1}{1 + T(z)} \quad (\text{A.22})$$

Where

$$T(z) = (1 + G_{RC}(z))G_c(z)G_p(z) \quad (\text{A.23})$$

Here $H(z)$ is taken as unity. From figure A.3 $G_{RC}(z)$ is given by:

$$G_{RC}(z) = \frac{z^{-N}Q(z)G_x(z)}{1 - z^{-N}Q(z)} \quad (\text{A.24})$$

Assuming $z^{-N}Q(z) = \beta$ gives:

$$G_{RC}(z) = \frac{\beta G_x(z)}{1 - \beta} \quad (\text{A.25})$$

Substituting $G_{RC}(z)$ in equation (A.23) gives:

$$T(z) = \left(1 + \frac{\beta G_x(z)}{1 - \beta}\right)G_c(z)G_p(z) \quad (\text{A.26})$$

Further simplification gives:

$$T(z) = \frac{1 + \beta(G_x(z) - 1)}{1 - \beta}G_c(z)G_p(z) \quad (\text{A.27})$$

Substituting (A.27) in (A.22) gives:

$$\frac{Y(z)}{V(z)} = \frac{1 - \beta}{1 + G_c(z)G_p(z) + G_c(z)G_p(z)\beta(G_x(z) - 1) - \beta} \quad (\text{A.28})$$

Taking $1 + G_c(z)G_p(z)$ as common from denominator gives:

$$\frac{Y(z)}{V(z)} = \frac{1 - \beta}{1 + G_c(z)G_p(z)} \times \frac{1}{1 + \frac{G_c(z)G_p(z)}{1 + G_c(z)G_p(z)}\beta(G_x(z) - 1) - \frac{\beta}{1 + G_c(z)G_p(z)}} \quad (\text{A.29})$$

Considering

$$T_{cl}(z) = \frac{G_c(z)G_p(z)}{1 + G_c(z)G_p(z)} \quad (\text{A.30})$$

Substituting (A.30) in (A.29) gives:

$$\frac{Y(z)}{V(z)} = \frac{1 - \beta}{1 + G_c(z)G_p(z)} \times \frac{1}{1 + T_{cl}(z)\beta(G_x(z) - 1) - \frac{\beta}{1 + G_c(z)G_p(z)}} \quad (\text{A.31})$$

Taking β as common in the denominator of second factor and further simplification gives:

$$\frac{Y(z)}{V(z)} = (1 - z^{-N}Q(z)) \times \frac{1}{1 + G_c(z)G_p(z)} \times \frac{1}{1 + (T_{cl}(z)G_x(z) - 1)z^{-N}Q(z)} \quad (\text{A.32})$$

A.5 Stability Conditions for Phase Lead Compensator

$$|(1 - M_{T_{cl}}(e^{j\Omega})e^{j\theta_{T_{cl}}(e^{j\Omega})}k_r e^{jm\Omega})M_Q(e^{j\Omega})e^{j\theta_Q(e^{j\Omega})}| < 1 \text{ for } 0 < \Omega < \pi \quad (\text{A.33})$$

All the frequency responses are functions of $e^{j\Omega}$. In the above equation, this is shown explicitly.

Dropping this notation makes the above expression simpler to deal with.

$$|(1 - M_{T_{cl}}k_r e^{j(m\Omega + \theta_{T_{cl}})})M_Q e^{j\theta_Q}| < 1 \text{ for } 0 < \Omega < \pi \quad (\text{A.34})$$

Introducing new variable β .

$$\beta = m\Omega + \theta_{T_{cl}} \quad (\text{A.35})$$

Substituting β in (A.34) gives:

$$|(1 - M_{T_{cl}}k_r e^{j\beta})M_Q e^{j\theta_Q}| < 1 \text{ for } 0 < \Omega < \pi \quad (\text{A.36})$$

Multiplication inside the parentheses gives:

$$|M_Q e^{j\theta_Q} - M_Q M_{T_{cl}} k_r e^{j(\beta + \theta_Q)}| < 1 \text{ for } 0 < \Omega < \pi \quad (\text{A.37})$$

As

$$e^{j\alpha} = \cos\alpha + j\sin\alpha \quad (\text{A.38})$$

Thus

$$\begin{aligned} |M_Q \cos\theta_Q + jM_Q \sin\theta_Q - M_Q M_{T_{cl}} k_r \cos(\beta + \theta_Q) \\ - jM_Q M_{T_{cl}} k_r \sin(\beta + \theta_Q)| < 1 \text{ for } 0 < \Omega < \pi \end{aligned} \quad (\text{A.39})$$

Taking the absolute value and squaring on both sides give:

$$\begin{aligned} [M_Q \cos\theta_Q - M_Q M_{T_{cl}} k_r \cos(\beta + \theta_Q)]^2 \\ + [M_Q \sin\theta_Q - M_Q M_{T_{cl}} k_r \sin(\beta + \theta_Q)]^2 < 1 \text{ for } 0 < \Omega < \pi \end{aligned} \quad (\text{A.40})$$

Squaring and combining terms give:

$$\begin{aligned} M_Q^2 + M_Q^2 M_{T_{cl}}^2 k_r^2 \\ - 2M_Q^2 M_{T_{cl}} k_r [\cos\theta_Q \cos(\beta + \theta_Q) + \sin\theta_Q \sin(\beta + \theta_Q)] < 1 \text{ for } 0 < \Omega < \pi \end{aligned} \quad (\text{A.41})$$

As

$$\cos(x - y) = \cos x \cos y + \sin x \sin y \quad (\text{A.42})$$

Thus

$$M_Q^2 + M_Q^2 M_{T_{cl}}^2 k_r^2 - 2M_Q^2 M_{T_{cl}} k_r \cos\beta < 1 \text{ for } 0 < \Omega < \pi \quad (\text{A.43})$$

Solving the inequality for K_r and substituting β from (A.35) gives:

$$0 < K_r < \frac{1 - M_Q^2}{M_Q^2 M_{T_{cl}}^2 k_r} + \frac{2\cos(m\Omega + \theta_{T_{cl}})}{M_{T_{cl}}} \text{ for } 0 < \Omega < \pi \quad (\text{A.44})$$

The first term on right hand side is a positive number as $0 \leq M_Q \leq 1$. Thus, the above condition is satisfied if the following conditions hold.

$$0 < K_r < \frac{2\cos(m\Omega + \theta_{T_{cl}})}{M_{T_{cl}}} \text{ for } 0 < \Omega < \pi \quad (\text{A.45})$$

$$0 \leq M_Q \leq 1 \text{ for } 0 < \Omega < \pi \quad (\text{A.46})$$

Also, for K_r to be positive following condition must be satisfied.

$$|m\Omega + \theta_{T_{cl}}| < 90^\circ \text{ for } 0 < \Omega < \pi \quad (\text{A.47})$$

A.6 Weights of Higher Order Generator

The higher order periodic signal generator is given by following equations.

$$G_{ho} = \frac{W(z)}{1 - W(z)} \quad (\text{A.48})$$

Where

$$W(z) = \sum_{l=1}^m w_l z^{-lN} \quad (\text{A.49})$$

m is the order of this periodic signal generator. w_l is the weight of l^{th} memory loop. These weights are computed by equating the frequency response of $W(e^{j\Omega})$ equal to 1 and its first $m - 1$ derivatives equal to 0. The frequency response of $W(z)$ is given by following equation.

$$W(e^{j\Omega}) = \sum_{l=1}^m w_l e^{-j\Omega lN} \quad (\text{A.50})$$

Where

$$\Omega = \omega T_s \quad (\text{A.51})$$

At tuned frequency; i.e. $f_p = \frac{1}{T_p}$; and its harmonics, Ω is given by:

$$\Omega = 2\pi k f_p T_s = \frac{2\pi k T_s}{T_p} = \frac{2\pi k}{N} \text{ where } k = 1, 2, 3, \dots \quad (\text{A.52})$$

Substituting (A.52) in (A.50) gives:

$$W(e^{j\Omega}) = \sum_{l=1}^m w_l (e^{-j2\pi})^{kl} \quad (\text{A.53})$$

As

$$e^{-j2\pi} = \cos 2\pi - j \sin 2\pi = 1 \quad (\text{A.54})$$

Thus (A.53) becomes:

$$W(e^{j\Omega}) = \sum_{l=1}^m w_l \quad (\text{A.55})$$

As infinite gain is required at the tuned frequency and its harmonics, equating (A.55) equal to 1 gives:

$$\sum_{l=1}^m w_l = 1 \quad (\text{A.56})$$

The derivative of $W(e^{j\Omega})$ with respect to Ω is given by:

$$\frac{\partial}{\partial \Omega} W(e^{j\Omega}) = \sum_{l=1}^m w_l e^{-j\Omega l N} (-j l N) \quad (\text{A.57})$$

Taking the value of (A.57) at $\Omega = \frac{2\pi k}{N}$ and equating it to zero gives:

$$-jN \sum_{l=1}^m w_l l = 0 \quad (\text{A.58})$$

Further simplification gives:

$$\sum_{l=1}^m w_l l = 0 \quad (\text{A.59})$$

The second derivative of $W(e^{j\Omega})$ with respect to Ω is given by:

$$\frac{\partial^2}{\partial \Omega^2} W(e^{j\Omega}) = \sum_{l=1}^m w_l e^{-j\Omega l N} (-j l N)^2 \quad (\text{A.60})$$

Taking the value of (A.60) at $\Omega = \frac{2\pi k}{N}$ and equating it to zero gives:

$$\sum_{l=1}^m w_l l^2 = 0 \quad (\text{A.61})$$

This result can be generalised for the $m - 1$ derivative.

$$\sum_{l=1}^m w_l l^{m-1} = 0 \quad (\text{A.62})$$

These results can be used to find optimal weights for higher order periodic signal generator of any order. In particular, for the m^{th} order generator, the weights can be found by using

following two formulae.

$$\sum_{l=1}^m w_l = 1 \quad (\text{A.63})$$

And

$$\sum_{l=1}^m w_l l^p = 0 \text{ for } p = 1, 2, 3, \dots, m - 1 \quad (\text{A.64})$$

For the second order generator, equations (A.63) and (A.64) give:

$$w_1 + w_2 = 1 \quad (\text{A.65})$$

And

$$w_1 + 2w_2 = 0 \text{ from } 1^{\text{st}} \text{ derivative} \quad (\text{A.66})$$

Solving these linear equations simultaneously, following weights are calculated.

$$w_1 = 2 \text{ and } w_2 = -1 \quad (\text{A.67})$$

Similarly, for the case of third order generator following equations are obtained.

$$w_1 + w_2 + w_3 = 1 \quad (\text{A.68})$$

And

$$w_1 + 2w_2 + 3w_3 = 0 \text{ from } 1^{\text{st}} \text{ derivative} \quad (\text{A.69})$$

$$w_1 + 4w_2 + 9w_3 = 0 \text{ from } 2^{\text{nd}} \text{ derivative} \quad (\text{A.70})$$

Thus, the weights are:

$$w_1 = 3, w_2 = -3 \text{ and } w_3 = 1 \quad (\text{A.71})$$

A.7 Stability of Higher Order Repetitive Controller

The sensitivity function for the system shown in figure A.4 is given by:

$$\frac{Y(z)}{V(z)} = \frac{1}{1 + T(z)} \quad (\text{A.72})$$

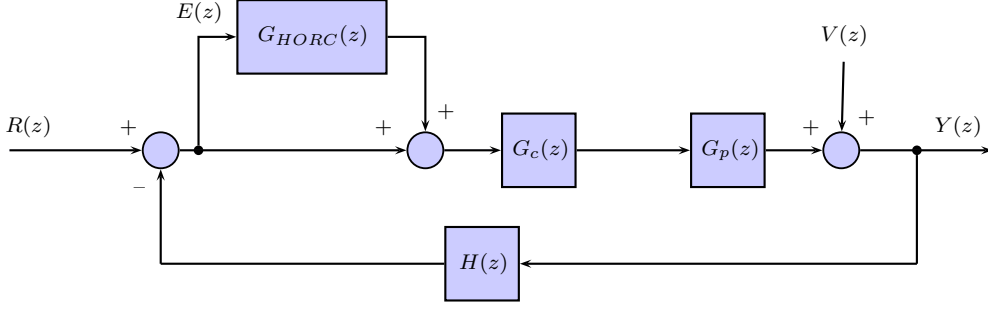


Figure A.4: Block diagram of generic close loop control system along with the plug-in higher order repetitive controller.

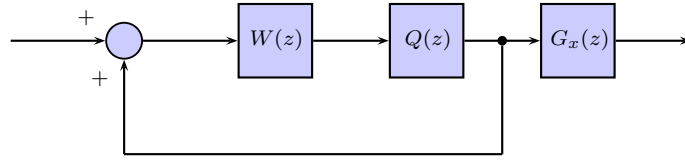


Figure A.5: Internal structure of higher order plug-in repetitive controller.

Where

$$T(z) = (1 + G_{HORC}(z))G_c(z)G_p(z) \quad (\text{A.73})$$

Here $H(z)$ is taken as unity. From figure A.5 $G_{HORC}(z)$ is given by:

$$G_{HORC}(z) = \frac{W(z)Q(z)G_x(z)}{1 - W(z)Q(z)} \quad (\text{A.74})$$

Where

$$W(z) = \sum_{l=1}^m w_l z^{-lN} \quad (\text{A.75})$$

Assuming $W(z)Q(z) = \beta$ gives:

$$G_{HORC}(z) = \frac{\beta G_x(z)}{1 - \beta} \quad (\text{A.76})$$

Substituting $G_{HORC}(z)$ in equation (A.73) gives:

$$T(z) = \left(1 + \frac{\beta G_x(z)}{1 - \beta}\right)G_c(z)G_p(z) \quad (\text{A.77})$$

Further simplification gives:

$$T(z) = \frac{1 + \beta(G_x(z) - 1)}{1 - \beta} G_c(z) G_p(z) \quad (\text{A.78})$$

Substituting (A.78) in (A.72) gives:

$$\frac{Y(z)}{V(z)} = \frac{1 - \beta}{1 + G_c(z)G_p(z) + G_c(z)G_p(z)\beta(G_x(z) - 1) - \beta} \quad (\text{A.79})$$

Taking $1 + G_c(z)G_p(z)$ as common from denominator gives:

$$\frac{Y(z)}{V(z)} = \frac{1 - \beta}{1 + G_c(z)G_p(z)} \times \frac{1}{1 + \frac{G_c(z)G_p(z)}{1 + G_c(z)G_p(z)}\beta(G_x(z) - 1) - \frac{\beta}{1 + G_c(z)G_p(z)}} \quad (\text{A.80})$$

Considering

$$T_{cl}(z) = \frac{G_c(z)G_p(z)}{1 + G_c(z)G_p(z)} \quad (\text{A.81})$$

Substituting (A.81) in (A.80) gives:

$$\frac{Y(z)}{V(z)} = \frac{1 - \beta}{1 + G_c(z)G_p(z)} \times \frac{1}{1 + T_{cl}(z)\beta(G_x(z) - 1) - \frac{\beta}{1 + G_c(z)G_p(z)}} \quad (\text{A.82})$$

Taking β as common in the denominator of second factor and further simplification gives:

$$\frac{Y(z)}{V(z)} = (1 - W(z)Q(z)) \times \frac{1}{1 + G_c(z)G_p(z)} \times \frac{1}{1 + (T_{cl}(z)G_x(z) - 1)W(z)Q(z)} \quad (\text{A.83})$$

A.8 Phase Lead Compensator for HORC

$$\|(T_{cl}(z)K_r z^m - 1)Q(z)W(z)\|_\infty < 1 \quad (\text{A.84})$$

Writing this condition in frequency domain and using the definition of infinity norm following inequality is obtained.

$$|(1 - M_{T_{cl}}(e^{j\Omega})e^{j\theta_{T_{cl}}(e^{j\Omega})}k_r e^{jm\Omega})M_Q(e^{j\Omega})e^{j\theta_Q(e^{j\Omega})}M_W(e^{j\Omega})e^{j\theta_W(e^{j\Omega})}| < 1 \text{ for } 0 < \Omega < \pi \quad (\text{A.85})$$

All the frequency responses are functions of $e^{j\Omega}$. In the above equation, this is shown explicitly. Dropping this notation makes the above expression simpler to deal with.

$$|(1 - M_{T_{cl}}k_r e^{j(m\Omega + \theta_{T_{cl}})})M_Q e^{j\theta_Q} M_W e^{j\theta_W}| < 1 \text{ for } 0 < \Omega < \pi \quad (\text{A.86})$$

Introducing new variable β .

$$\beta = m\Omega + \theta_{T_{cl}} \quad (\text{A.87})$$

Substituting β in (A.86) gives:

$$|(1 - M_{T_{cl}}k_r e^{j\beta})M_Q e^{j\theta_Q} M_W e^{j\theta_W}| < 1 \text{ for } 0 < \Omega < \pi \quad (\text{A.88})$$

Multiplication inside the parentheses gives:

$$|M_Q M_W e^{j\theta_Q} e^{j\theta_W} - M_Q M_W M_{T_{cl}} k_r e^{j(\beta + \theta_Q + \theta_W)}| < 1 \text{ for } 0 < \Omega < \pi \quad (\text{A.89})$$

As

$$e^{j\alpha} = \cos\alpha + j\sin\alpha \quad (\text{A.90})$$

Thus

$$\begin{aligned} &|M_Q M_W \cos(\theta_Q + \theta_W) + jM_Q M_W \sin(\theta_Q + \theta_W) - M_Q M_W M_{T_{cl}} k_r \cos(\beta + \theta_Q + \theta_W) \\ &\quad - jM_Q M_W M_{T_{cl}} k_r \sin(\beta + \theta_Q + \theta_W)| < 1 \text{ for } 0 < \Omega < \pi \quad (\text{A.91}) \end{aligned}$$

Taking the absolute value and squaring on both sides give:

$$\begin{aligned} &[M_Q M_W \cos(\theta_Q + \theta_W) - M_Q M_W M_{T_{cl}} k_r \cos(\beta + \theta_Q + \theta_W)]^2 + [M_Q M_W \sin(\theta_Q + \theta_W) \\ &\quad - M_Q M_W M_{T_{cl}} k_r \sin(\beta + \theta_Q + \theta_W)]^2 < 1 \text{ for } 0 < \Omega < \pi \quad (\text{A.92}) \end{aligned}$$

Squaring and combining terms give:

$$M_Q^2 M_W^2 + M_Q^2 M_W^2 M_{T_{cl}}^2 k_r^2 - 2M_Q^2 M_W^2 M_{T_{cl}} k_r [\cos(\theta_Q + \theta_W) \cos(\beta + \theta_Q + \theta_W) + \sin(\theta_Q + \theta_W) \sin(\beta + \theta_Q + \theta_W)] < 1 \text{ for } 0 < \Omega < \pi \quad (\text{A.93})$$

As

$$\cos(x - y) = \cos x \cos y + \sin x \sin y \quad (\text{A.94})$$

Thus

$$M_Q^2 M_W^2 + M_Q^2 M_W^2 M_{T_{cl}}^2 k_r^2 - 2M_Q^2 M_W^2 M_{T_{cl}} k_r \cos \beta < 1 \text{ for } 0 < \Omega < \pi \quad (\text{A.95})$$

Solving the inequality for K_r and substituting β from (A.86) gives:

$$0 < K_r < \frac{1 - M_Q^2 M_W^2}{M_Q^2 M_W^2 M_{T_{cl}}^2 k_r} + \frac{2\cos(m\Omega + \theta_{T_{cl}})}{M_{T_{cl}}} \text{ for } 0 < \Omega < \pi \quad (\text{A.96})$$

As $M_W^2 \gg 1$, thus (A.96) becomes

$$0 < K_r < \frac{-M_Q^2 M_W^2}{M_Q^2 M_W^2 M_{T_{cl}}^2 k_r} + \frac{2\cos(m\Omega + \theta_{T_{cl}})}{M_{T_{cl}}} \text{ for } 0 < \Omega < \pi \quad (\text{A.97})$$

Simplification gives:

$$0 < K_r < \frac{-1}{M_{T_{cl}}^2 k_r} + \frac{2\cos(m\Omega + \theta_{T_{cl}})}{M_{T_{cl}}} \text{ for } 0 < \Omega < \pi \quad (\text{A.98})$$

Only considering the right hand inequality.

$$K_r < \frac{-1}{M_{T_{cl}}^2 k_r} + \frac{2\cos(m\Omega + \theta_{T_{cl}})}{M_{T_{cl}}} \text{ for } 0 < \Omega < \pi \quad (\text{A.99})$$

Rearranging terms give:

$$K_r^2 - \frac{2\cos(m\Omega + \theta_{T_{cl}})}{M_{T_{cl}}} K_r + \frac{1}{M_{T_{cl}}^2} < 0 \text{ for } 0 < \Omega < \pi \quad (\text{A.100})$$

This is a quadratic inequality. It can be solved by solving the corresponding quadratic equation which is:

$$K_r^2 - \frac{2\cos(m\Omega + \theta_{T_{cl}})}{M_{T_{cl}}}K_r + \frac{1}{M_{T_{cl}}^2} = 0 \text{ for } 0 < \Omega < \pi \quad (\text{A.101})$$

The roots of K_r from this equation are:

$$K_r = \frac{1}{M_{T_{cl}}} \left[\cos(m\Omega + \theta_{T_{cl}}) \pm \sqrt{\cos^2(m\Omega + \theta_{T_{cl}}) - 1} \right] \text{ for } 0 < \Omega < \pi \quad (\text{A.102})$$

For very small values of $m\Omega + \theta_{T_{cl}}$, $\sqrt{\cos^2(m\Omega + \theta_{T_{cl}}) - 1} = 0$. Thus following condition is introduced.

$$|m\Omega + \theta_{T_{cl}}| = 0^\circ \text{ for } 0 < \Omega < \pi \quad (\text{A.103})$$

Under this condition, (A.102) becomes:

$$K_r = \frac{\cos(m\Omega + \theta_{T_{cl}})}{M_{T_{cl}}} \text{ for } 0 < \Omega < \pi \quad (\text{A.104})$$

And the corresponding inequality is:

$$K_r < \frac{\cos(m\Omega + \theta_{T_{cl}})}{M_{T_{cl}}} \text{ for } 0 < \Omega < \pi \quad (\text{A.105})$$

Appendix B

Elucidation of Concepts

B.1 Input Output Stability

Input output stability deals with the stability of systems from the perspective of input and output instead of looking into the system. A system is said to be input output stable (IOS) if its output is bounded for all bounded inputs. This is also called BIBO stability. Following sections describe various forms and formulas for BIBO stability.

B.1.1 H_∞ Stability

Infinity norm, H_∞ , of a system $G(s)$ is given by:

$$\|G(s)\|_\infty = \max_{\omega} |G(j\omega)| \quad (\text{B.1})$$

Thus, H_∞ is the peak gain of $G(s)$ and can be found by analysing the bode plot of $G(s)$. H_∞ stability of a system is defined by following theorem.

Theorem 6 *A LTI system defined by gain function $G(s)$ is H_∞ stable if*

$$\max_{\omega} |G(j\omega)| < \infty$$

This theorem guarantees BIBO stability of a system. A system which has finite H_∞ norm produces finite output for every finite input.

B.1.2 Small Gain Theorem

Small gain theorem is a very general result[25]. It is applicable to both linear and non-linear systems. However, it must be kept in mind that this theorem is a sufficient condition for stability. It means that if this theorem holds for a system, then that system is stable. But if this theorem does not hold true, then the system can be stable or unstable.

Theorem 7 *The close-loop system given in figure B.1 is stable if*

1. $H_1(s)$ and $H_2(s)$ are H_∞ stable
2. $\|H_1(s)\|_\infty \times \|H_2(s)\|_\infty < 1$

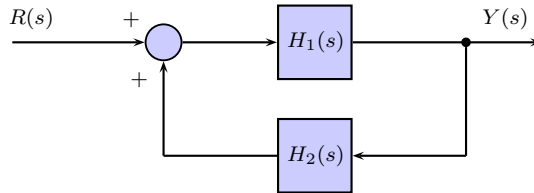


Figure B.1: Block diagram of close-loop system.

The conditions of this theorem are simple and intuitive. The first condition demands H_∞ stability of both subsystems $H_1(s)$ and $H_2(s)$. This means that these systems should produce bounded outputs for bounded inputs. The second condition makes the first condition redundant, as the product can only be finite if the multiplicands are finite. The second condition can be understood by considering the following input output relation.

$$Y(s) = \frac{H_1(s)}{1 - H_1(s)H_2(s)} \times R(s) \quad (\text{B.2})$$

If small gain theorem is satisfied, then $H_1(s)H_2(s) < 1$. Equation (B.2) becomes:

$$Y(s) = H_1(s)R(s) \quad (\text{B.3})$$

As $H_1(s)$ is H_∞ stable, thus the close-loop system is BIBO stable. This simple argument shows that if small gain theorem holds, BIBO stability is guaranteed.

Now, Let's consider that the small gain theorem is not satisfied for the system in figure B.1 and $H_1(s)H_2(s) \geq 1$. In this case, equation (B.2) becomes:

$$Y(s) = \frac{1}{H_2(s)} \times R(s) \quad (\text{B.4})$$

Now the input output stability depends on the inverse of $H_2(s)$. If $H_2(s)$ is unity, then the system is IOS. However, if $H_2(s)$ has close to zero gain at high frequencies, then its inverse has infinite gain at high frequencies which makes the system unstable. Therefore, if the small gain theorem is not satisfied, it does not mean that the system is unstable. This is the very reason small gain theorem is a sufficient condition for stability.

Bibliography

- [1] G. A. Ramos, R. Costa-Castelló, and J. M. Olm, *Digital repetitive control under varying frequency conditions*, vol. 446. Springer, 2013.
- [2] B. A. Francis and W. M. Wonham, “The internal model principle of control theory,” *Automatica*, vol. 12, no. 5, pp. 457–465, 1976.
- [3] R. Teodorescu, F. Blaabjerg, M. Liserre, and P. C. Loh, “Proportional-resonant controllers and filters for grid-connected voltage-source converters,” *IEE Proceedings-Electric Power Applications*, vol. 153, no. 5, pp. 750–762, 2006.
- [4] T. Inoue, M. Nakano, and S. Iwai, “High accuracy control of servomechanism for repeated contouring,” in *Proceedings of the 10th Annual Symposium on Incremental Motion Control Systems and Devices*, pp. 285–292, 1981.
- [5] T. Inoue, M. Nakano, T. Kubo, S. Matsumoto, and H. Baba, “High accuracy control of a proton synchrotron magnet power supply,” in *Proceedings of the 8th World Congress of IFAC*, vol. 20, pp. 216–221, 1981.
- [6] S. Hara, T. Omata, and M. Nakano, “Synthesis of repetitive control systems and its application,” in *Decision and Control, 1985 24th IEEE Conference on*, pp. 1387–1392, IEEE, 1985.
- [7] S. Hara, Y. Yamamoto, T. Omata, and M. Nakano, “Repetitive control system: a new type servo system for periodic exogenous signals,” *Automatic Control, IEEE Transactions on*, vol. 33, no. 7, pp. 659–668, 1988.
- [8] T. Inoue, “Practical repetitive control system design,” in *Decision and Control, 1990., Proceedings of the 29th IEEE Conference on*, pp. 1673–1678, IEEE, 1990.

- [9] M.-C. Tsai and W.-S. Yao, “Design of a plug-in type repetitive controller for periodic inputs,” *Control Systems Technology, IEEE Transactions on*, vol. 10, no. 4, pp. 547–555, 2002.
- [10] K. Srinivasan and F.-R. Shaw, “Analysis and design of repetitive control systems using the regeneration spectrum,” *Journal of dynamic systems, measurement, and control*, vol. 113, no. 2, pp. 216–222, 1991.
- [11] R. Griñó and R. Costa-Castelló, “Digital repetitive plug-in controller for odd-harmonic periodic references and disturbances,” *Automatica*, vol. 41, no. 1, pp. 153–157, 2005.
- [12] B. Zhang, K. Zhou, Y. Wang, and D. Wang, “Performance improvement of repetitive controlled pwm inverters: A phase-lead compensation solution,” *International Journal of Circuit Theory and Applications*, vol. 38, no. 5, pp. 453–469, 2010.
- [13] D. Wang and Y. Ye, “Design and experiments of anticipatory learning control: Frequency-domain approach,” *Mechatronics, IEEE/ASME Transactions on*, vol. 10, no. 3, pp. 305–313, 2005.
- [14] G. Ramos, J. M. Olm, R. Costa-Castelló, *et al.*, “Repetitive control of an active filter under varying network frequency: Power factor correction,” in *Robotics Symposium, 2011 IEEE IX Latin American and IEEE Colombian Conference on Automatic Control and Industry Applications (LARC)*, pp. 1–5, IEEE, 2011.
- [15] E. Kurniawan, Z. Cao, and Z. Man, “Design of robust repetitive control with time-varying sampling periods,” *Industrial Electronics, IEEE Transactions on*, vol. 61, no. 6, pp. 2834–2841, 2014.
- [16] M. Steinbuch, “Repetitive control for systems with uncertain period-time,” *Automatica*, vol. 38, no. 12, pp. 2103–2109, 2002.
- [17] G. Pipeleers, B. Demeulenaere, J. D. Schutter, and J. Swevers, “Robust high-order repetitive control,” in *American Control Conference, 2008*, pp. 1080–1085, IEEE, 2008.

- [18] G. Ramos, J. M. Olm, R. Costa-Castelló, *et al.*, “Digital repetitive control under time-varying sampling period: An lmi stability analysis,” in *Control Applications,(CCA) & Intelligent Control,(ISIC), 2009 IEEE*, pp. 782–787, IEEE, 2009.
- [19] G. Ramos, R. Costa-Castelló, J. M. Olm, R. Cardoner, *et al.*, “Robust high-order repetitive control of an active filter using an odd-harmonic internal model,” in *Industrial Electronics (ISIE), 2010 IEEE International Symposium on*, pp. 1040–1045, IEEE, 2010.
- [20] S. Abu-Sharkh, R. Arnold, J. Kohler, R. Li, T. Markvart, J. Ross, K. Steemers, P. Wilson, and R. Yao, “Can microgrids make a major contribution to uk energy supply?,” *Renewable and Sustainable Energy Reviews*, vol. 10, no. 2, pp. 78–127, 2006.
- [21] M. Jamil, B. Hussain, S. Sharkh, M. Abu-Sara, and R. Boltryk, “Microgrid power electronic converters: State of the art and future challenges,” 2009.
- [22] S. M. Abu Sharkh and M. A. Abu-Sara, “Current control of utility-connected two-level and three-level pwm inverters,” *European Power Electronics and Drives Journal*, vol. 14, no. 3, pp. 13–18, 2004.
- [23] M. Jamil, *Repetitive current control of two-level and interleaved three-phase PWM utility connected converters*. PhD thesis, University of Southampton, 2012.
- [24] I. F II, “Ieee recommended practices and requirements for harmonic control in electrical power systems,” 1993.
- [25] C. A. Desoer and M. Vidyasagar, *Feedback systems: input-output properties*, vol. 55. SIAM, 1975.